ไมโคร/นาโนสเฟียร์จากพอลิซิลเซสควิออกเซนที่มีหมู่ดูดกลืนยูวีเอ

นางสาวพรรณนิภา กฤษณีไพบูลย์

วิทยานิพนธ์นี้เป็นส่วนหนึ่งของการศึกษาตามหลักสูตรปริญญาวิทยาศาสตรมหาบัณฑิต
สาขาวิชาเคมี ภาควิชาเคมี
คณะวิทยาศาสตร์ จุฬาลงกรณ์มหาวิทยาลัย
ปีการศึกษา 2552
ลิขสิทธิ์ของจุฬาลงกรณ์มหาวิทยาลัย

MICRO/NANOSPHERES FROM POLYSILSESQUIOXANE CONTAINING UVA-ABSORBING GROUP

Miss Punnipa Kidsaneepoiboon

A Thesis Submitted in Partial Fulfillment of the Requirements
for the Degree of Master of Science Program in Chemistry
Department of Chemistry
Faculty of Science
Chulalongkorn University
Academic Year 2009
Copyright of Chulalongkorn University

Thesis Title	MICRO/NANOSPHERES FROM POLYSILSESQUIOXANE CONTAINING UVA-ABSORBING GROUP
By	Miss Punnipa Kidsaneepoiboon
Field of Study	Chemistry
Thesis Advisor	Associate Professor Supason Wanichwecharungruang,Ph.D.

Accepted by the Faculty of Science, Chulalongkorn University in Partial Fulfillment of the Requirements for the Master's Degree

……Dean of the Faculty of Science
(Professor Supot Hannongbua, Dr.rer.nat.)

THESIS COMMITTEE

…….. Chairman
(Associate Professor Dr. Sirirat Kokpol, Ph.D.)

……..……. Thesis Advisor
(Associate Professor Supason Wanichwecharungruang, Ph.D.)

…….. Examiner
(Sumrit Wacharasindhu, Ph.D.)

…….. External Examiner
(Veerapat Tantayakom, Ph.D.)

พรรณนิภา กฤษณีไพบูลย์: ไมโคร/นาโนสเฟียร์จากพอลิซิลเซสควิออกเซนที่มีหมู่ดูดกลืนยูวีเอ (MICRO/NANOSPHERES FROM POLYSILSESQUIOXANE CONTAINING UVA-ABSORBING GROUP) อ. ที่ปรึกษาวิทยานิพนธ์หลัก: รศ. ดร. ศุภศร วนิชเวชารุ่งเรือง, 74 หน้า.

งานวิจัยนี้ได้เตรียมไมโคร/นาโนสเฟียร์ของสารพอลิซิลเซสควิออกเซนที่มีสมบัติการดูดกลืนยูวีได้สำเร็จจากปฏิกิริยาพอลิเมอไรเซชันของมอนอเมอร์ไตรเอททอกซีไซลิลโพรพิล-4-เมททอกซีซินนามาไมด์ และไตรเอททอกซีไซลิลโพรพิล-2,4-ไดเมททอกซีซินนาไมด์ โดยพบว่าชนิดของตัวเร่งปฏิกิริยาและปริมาณของตัวทำละลายในระหว่างการสร้างอนุภาคมีผลต่อขนาดอนุภาคและปริมาณของผลิตภัณฑ์ที่ได้ ขนาดอนุภาคเพิ่มขึ้นเมื่อมีการเพิ่มปริมาณตัวทำละลาย แต่ปริมาณของตัวทำละลายที่สูงจะมีผลสวนทางกับปริมาณของผลิตภัณฑ์ที่ได้ นอกจากนี้ปฏิกิริยาพอลิเมอไรซ์เซชันของโมโนเมอร์ที่ความเข้มข้นสูงมีผลทำให้ปริมาณของผลิตภัณฑ์ที่ได้ลดลง การกักเก็บ 2-เอททิลเฮกซิล-4-เมททอกซีซินนาเมทในอนุภาคพอลิโพรพิล-4-เมททอกซีซินนามาไมด์ซิลเซสควิออกเซน และอนุภาคพอลิโพรพิล-2,4-ไดเมททอกซีซินนามาไมด์ซิลเซสควิออกเซน ให้ประสิทธิภาพในการกักเก็บที่ 61.54 เปอร์เซ็นต์ (ที่ความสามารถในการบรรจุ 20.86 เปอร์เซ็นต์) และ 31.87 เปอร์เซ็นต์ (ที่ความสามารถในการบรรจุ 10.17 เปอร์เซ็นต์) ตามลำดับ

ภาควิชา.....เคมี.....ลายมือชื่อนิสิต.....
สาขาวิชา.....เคมี.....ลายมือชื่อ อ.ที่ปรึกษาวิทยานิพนธ์หลัก.....
ปีการศึกษา .....2552.....

5072379123 : MAJOR CHEMISTRY

KEYWORDS : Polysilsesquioxane / Nanoparticles / UV filter

PUNNIPA KIDSANEEPOIBOON: MICRO/NANOSPHERES FROM POLYSILSESQUIOXANE CONTAINING UVA-ABSORBING GROUP THESIS ADVISOR: ASSOC. PROF. SUPASON WANICHWECHARUNGRUANG, Ph.D., 74 pp.

In this research, we prepared polysilsesquioxane micro/nanospheres with UV absorption property through the polymerization process of hybrid monomer, triethoxysilylpropyl-4-methoxycinnamamide and triethoxysilylpropyl-2,4-dimethoxycinnamamide. It was found that the catalysis types and volume of solvent used during the particle formation, affected particle size and product yield. Particle size increased with the increased volume of solvent but the high volume of solvent inversely correlated with product yield. Moreover, polymerization at higher monomer concentration gave a lower yield. Encapsulation of 2-ethylhexyl-4-methoxycinnamate into poly[propyl-4-methoxycinnamamide silsesquioxane], PTES4C and poly[propyl-2,4-dimethoxycinnamamide silsesquioxane], PTES24C spherical particles could be carried out successfully at 61.54% encapsulation efficiency (20.86% loading) and 31.87% encapsulation efficiency (10.17% loading), respectively.

Department : Chemistry Student's Signature .....

Field of Study : Chemistry Advisor's Signature .....

Academic Year : 2009

ACKNOWLEDGEMENTS

I have many people to thank for their help and encouragement for this project. First of all, I would like to express my deeply – say many thanks to my beloved advisor, Associate Professor Dr. Supason Wanichwecharungruang, for all her valuable suggestion, guidance, encouragement all throughout my study.

I am also grateful to the other member of my committee, Associate Professor Dr. Sirirat Kokpol, Dr. Sumrit Wacharasindhu and Dr. Veerapat Tantayakom for their comments, technical guidelines and advice given to me for the completion of my thesis work.

I am also special acknowledge Center for Petroleum, Petrochemicals, and Advanced Materials.

Moreover, I also special acknowledge all members of research group for the good working environment, helpful, opinion and encouragement.

Most importantly, I would like to express my deepest gratitude to my parent and relatives for their love, continued help, support, encouragement and endless patience they always give me. Without all of them as mentioned, this thesis would not be possible.

CONTENTS

Page

Abstract in Thai…… iv
Abstract in English…… v
Acknowledgements…… vi
List of Tables…… x
List of Figures…… xi
List of Schemes …… xvii
List of Abbreviations…… xviii
CHAPTER I INTRODUCTION…… 1
Silsesquioxane…… 1
3-Aminopropyltriethoxysilane…… 4
Cinnamic acid derivative…… 7
1.1 Literature reviews…… 8
1.2 Research goal…… 14
CHAPTER II EXPERIMENTAL…… 15
2.1 Materials and Chemicals…… 15
2.2 Instruments and Equipments…… 15
2.3 Synthesis of 2,4-dimethoxycinnamic acids…… 16
2.4 Synthesis of hybrid monomers…… 17
2.5 Micro/nanoparticles formation…… 20
2.5.1 Poly[propyl-4-methoxycinnamamidesilsesquioxane] (PTES4C) products…… 21
2.5.2 Poly[propyl-2,4-dimethoxycinnamamidesilsesquioxane] (PTES24C) products…… 22
2.6 Effect of an added surfactant…… 25
2.7 Encapsulation process…… 25
2.8 Particle size, SEM and TEM analyses…… 26
CHAPTER III RESULT AND DISCUSSION…… 27
3.1 Hybrid monomers…… 27

Page

3.1.1 Synthesis of triethoxysilylpropyl-4-methoxycinnamamide (TES4C) hybrid monomers…….. 27
3.1.2 Synthesis of triethoxysilylpropyl-2,4-dimethoxycinnamamide (TES24C) hybrid monomers…… 30
3.2 Polymerization and micro/nanospheres formation…… 33
3.2.1 Poly[propyl-4-methoxycinnamamidesilsesquioxane] (PTES4C) spheres…….. 34
3.2.2 Poly[propyl-2,4-dimethoxycinnamamidesilsesquioxane] (PTES24C) spheres…….. 38
3.2.3 Polymerization mechanism……...…… 42
3.3 Effects of monomer concentration during the particle formation ……. 47
3.3.1 Poly[propyl-4-methoxycinnamamidesilsesquioxane] (PTES4C) sphere……... 47
3.3.2 Poly[propyl-2,4-dimethoxycinnamamidesilsesquioxane] (PTES24C) sphere……..... 48
3.4 Effects of surfactant…… 49
3.5 Encapsulation processes…… 51
3.5.1 Encapsulation of 2-ethylhexyl-4-methoxycinnamate into poly[propyl-4-methoxycinnamamidesilsesquioxane] (PTES4C) spheres…… 52
3.5.2 Encapsulation of 2-ethylhexyl-4-methoxycinnamate into poly[propyl-2,4-dimethoxycinnamamidesilsesquioxane] (PTES24C) spheres…… 53
3.6 Measurement of a solar protection factor (SPF)……. 54
3.7 Redispersion and particle stability from various catalysts…..……... 55
CHAPTER IV CONCLUSION…….…… 57
REFERENCES……... 58

Page

APPENDICES……..... 62
APPENDIX A……...……..... 63
APPENDIX B…..……...……..... 70
VITA……... 74

List of Tables

		Page
Table 1.1	Summary of physicochemical properties……	5
Table 1.2	Summary of stability in water properties……	6
Table 1.3	Summary of LD_{50} values……	7
Table 2.1	Condition used during the syntheses of hybrid monomers…….	17
Table 2.2	Condition used during the syntheses poly[propyl-4-methoxy cinnamamidesilsesquioxane] **(PTES4C)** nanospheres…….	23
Table 2.3	Condition used during the syntheses poly[propyl-2,4-dimethoxy cinna-mamidesilsesquioxane] **(PTES24C)** nanospheres……..	24
Table 3.1	Particle characteristics of the synthesized poly[propyl-4-methoxy cinnamamidesilsesquioxane] **(PTES4C)** obtained from various catalysis processes, e.g. 0.1% HCl, self-catalysis, 3% NH_4OH and 5% NH_4OH with the ethanol effect (20%, 30% and 40% (v/v))……...	35
Table 3.2	Particle characteristics of the synthesized poly[propyl-2,4-dimethoxy cinnamamidesilsesquioxane] **(PTES24C)** obtained from various catalysis processes, e.g. 0.1% HCl, self-catalysis, 3% NH_4OH and 5% NH_4OH with the ethanol effect (10%, 20% and 30% (v/v))……	39
Table 3.3	Characteristics of **PTES4C** particles prepared at different monomer concentration……..	47
Table 3.4	Characteristics of **PTES24C** particles prepared at different monomer concentration……..	48
Table 3.5	The solar protection factor (SPF) and UV-A protection factor (UV-A PF) values of poly[propyl-4-methoxycinnamamide silsesquioxane] **(PTES4C)**, poly[propyl-2,4-dimethoxy cinnamamidesilsesquioxane] **(PTES24C)** and 2-ethyl-hexyl-4-trimethoxycinnamate **(EHMC)**……...	54

List of Figures

Page

Figure 1.1	Hydrolytic condensation reactions of trifunctional organo-silicon monomers……..…..	2
Figure 1.2	T8 cage (closed cubic) structures……..	3
Figure 1.3	Synthesis of silsesqiuoxanes are usually formed via poly-condensation of trifunctional silanes……..	3
Figure 1.4	Structural Formula of 3-aminopropyltriethoxysilane……...	4
Figure 1.5	Synthetic pathway of 3-aminopropyltriethoxysilane (APTES)……...	5
Figure 1.6	Structure of hydrolytically stable bond from APTES……....	6
Figure 1.7	Electron micrograph of silica spheres obtained in the ethanol-ethyl ester system (a) and tetrapentyl silicate in a 3:1 propanol-methanol mixture (b)……...…….	8
Figure 1.8	Scanning electron micrograph of organo-silica powders which are prepared PTMS(a), MTMS(b) and MTES(c)…….	9
Figure 1.9	Scanning electron micrograph of particles obtained from VTS and comonomer (APTES) (a). Proposed steric and charge stabilization by APTES (b)……	9
Figure 1.10	Scanning electron micrograph of OMC containing micro-capsules and a rare open microcapsule……	10
Figure 1.11	Scanning electron micrograph of polysilsesquioxane spherical particle containing UVB filter……...……...	10
Figure 1.12	Structure of hybrid organic-inorganic nanoballs blockcopolymers……...…….……..	11
Figure 1.13	Structure of 1,1’-bis[3-(trimethoxysilyl)propyl]-4,4’-bipyridinium Iodide bridged polysilsesquioxane (left) and N,N’-bis[(3-trimethoxysilyl) propyl]ethylenediamine bridged polysilsesquioxane (right)…….	11

Page

Figure 1.14	Structure of modified chitosan films…….	12
Figure 1.15	Scanning electron microscope images of the silica micro-capsules formed at an impeller speed of 1,200 (a). The encapsulation precursor prepared in H_2O/TEOS=1.7. THBP was used as the hydrophilic active compound (b)……	13
Figure 1.16	Scanning electron microscope images of particles from poly(methyl methacrylate) containing BMDBMA and 2-ethylhexyl-4-methoxycinnamate……...	13
Figure 2.1	Particles formation processes of **TES4C**……..	21
Figure 2.2	Particles formation processes of **TES24C**……	22
Figure 3.1	^{1}H-NMR spectrum and structure of triethoxysilylpropyl-4-methoxy cinnamamide, (**TES4C-1**, (a) and **TES4C-2**, (b)) in $CDCl_3$……..……..	28
Figure 3.2	FT-IR spectra of 3-aminopropyltriethoxysilane **(APTES)** (a), 4-methoxycinnamic acid (b) and triethoxysilylpropyl-4-methoxy cinnamamide, **(TES4C-1)** (c)……...	29
Figure 3.3	UV absorption spectrum of **TES4C-2** at molar absorptivity 1.31 x 10-5 M……...……	30
Figure 3.4	^{1}H-NMR spectrum and structure of triethoxysilylpropyl-4-methoxy cinnamamide, (**TES24C-1**, (a) and **TES24C-2**, (b)) in $CDCl_3$……..…	31
Figure 3.5	FT-IR spectra of 3-aminopropyltriethoxysilane **(APTES)** (a), 2,4-dimethoxycinnamic acid (b) and triethoxysilylpropyl-2,4-dimethoxycinnamamide, **(TES24C-1)** (c)…….	32
Figure 3.6	UV absorption spectrum of **TES24C-2** at molar absorptivity 1.24 x 10-5 M……...	33

Page

Figure 3.7	The synthesis yields (%) of poly[propyl-4-methoxycinna-mamidesilsesquioxane] **(PTES4C)** in various catalysis processes, e.g. 0.1% HCl, self-catalyst, 3% NH_4OH and 5% NH_4OH with the ethanol effect (20%, 30% and 40% (v/v))	36
Figure 3.8	UV absorption spectrum of 80 ppm (in 20% ethanol) of **PTES4C** suspension product, **(a)** and 10 mg of **PTES4C** solid product, **(b)**……..	37
Figure 3.9	The synthesis yields (%) of poly[propyl-2,4-dimethoxy cinnamamidesilsesquioxane] **(PTES24C)** in various catalysis processes, e.g. 0.1% HCl, self-catalyst, 3% NH_4OH and 5% NH_4OH with the ethanol effect (10%, 20% and 30% (v/v))…….....…….	40
Figure 3.10	UV absorption spectrum of 200 ppm (in 20% ethanol) of **PTES24C** suspension product, **(a)** and 10 mg of **PTES24C** solid product, **(b)**……..	41
Figure 3.11	Proposed mechanism for the acid catalyst hydrolysis…...…...	42
Figure 3.12	Proposed mechanism for the base catalyst hydrolysis…….....	43
Figure 3.13	Proposed mechanism for the self-catalyst hydrolysis…….....	44
Figure 3.14	Polycondensation reactions of silanol molecules through water-condensation and alcohol-condensation…….	45
Figure 3.15	Proposed mechanism for ethanol affects to polymerization processes……...	46
Figure 3.16	Scanning electron micrographs of **PTES4C** spheres prepared at the concentrations of 0.02 g/ml (a), 0.04 g/ml (b) and 0.06 g/ml (c)…….……	48
Figure 3.17	Scanning electron micrographs of **PTES24C** spheres prepared at the concentrations of 0.02 g/ml (a), 0.04 g/ml (b) and 0.06 g/ml (c)……...……...	49

Page

Figure 3.18	Pictures of **PTES4C** products obtained with (a, left) and with out (a, right) the presence of Triton X-100 in the preparation process. SEM photographs of **PTES4C** obtained with (b) and with out (c) Triton X-100…….....	50
Figure 3.19	Pictures of **PTES24C** products obtained with (a, left) and with out (a, right) the presence of Triton X-100 in the preparation process. SEM photographs of **PTES24C** obtained with (b) and with out (c) Triton X-100……..	51
Figure 3.20	Morphology of non-encapsulated **PTES4C** particles (a, b) and **EHMC**-encapsulated **PTES4C** particles (c, d). The images were obtained by SEM (a, c) and TEM (b, d)……..	52
Figure 3.21	SEM images of non-encapsulated **PTES24C** particles (a), **EHMC**-encapsulated **PTES24C** particles (b) and **EHMC**-encapsulated **PTES24C** particles in a presence of surfactant (c)…….	53
Figure 3.22	The creams containing poly[propyl-4-methoxy cinnamamidesilsesquioxane] **(PTES4C)**(a), poly[propyl-2,4-dimethoxycinnamamide silsesqui oxane] **(PTES24C)** (b) and 2-ethyl-hexyl-4-trimethoxycinnamate **(EHMC)** (c)…….	54
Figure 3.23	Pictures of the redispersed **PTES4C** particles prepared at0.01 g/ml…….	55
Figure 3.24	Pictures of the redispersed **PTES24C** particles prepared at0.01 g/ml…….	56
Figure A1	IR (a) and ^{1}H-NMR spectrum (b) of 2,4-dimethoxycinnamic acid **(2,4-DMC)** in $CDCl_3$……	63
Figure A2	IR (a) and ^{1}H-NMR spectrum (b) of 3-aminopropyltriethoxy silane **(APTES)** in $CDCl_3$……	64
Figure A3	IR (a) of triethoxysilylpropyl-4-methoxycinnamamide, DS=0.8 **(TES4C-2)** in $CDCl_3$……..….	65

Page

Figure A4	IR (a) of triethoxysilylpropyl-2,4-dimethoxycinnamamide, DS=0.78 **(TES24C-2)** in $CDCl_3$……..	66
Figure A5	Scanning electron micrographs of **PTES4C** spheres prepared under self-catalytic process at 0.02 g/ml monomer concentration with the ethanol percentages of 20% (v/v) (a), 30% (v/v) (b) and 40% (v/v) (c)……	67
Figure A6	Scanning electron micrographs of **PTES4C** spheres prepared under 0.1% HCl catalytic process at 0.02 g/ml monomer concentration with the ethanol percentages of 20% (v/v) (a), 30% (v/v) (b) and 40% (v/v) (c)……..	67
Figure A7	Scanning electron micrographs of **PTES4C** spheres prepared under 3% NH_4OH catalytic process at 0.02 g/ml monomer concentration with the ethanol percentages of 20% (v/v) (a), 30% (v/v) (b) and 40% (v/v) (c)……..	68
Figure A8	Scanning electron micrographs of **PTES4C** spheres prepared under 5% NH_4OH catalytic process at 0.02 g/ml monomer concentration with the ethanol percentages of 20% (v/v) (a), 30% (v/v) (b) and 40% (v/v) (c)……...	68
Figure A9	Scanning electron micrographs of **PTES24C** spheres prepared under 0.1% HCl catalytic process at 0.02 g/ml monomer concentration with the ethanol percentages of 10% (v/v) (a), 20% (v/v) (b) and 30% (v/v) (c)……...	68
Figure A10	Scanning electron micrographs of **PTES24C** spheres prepared under self-catalytic catalytic process at 0.02 g/ml monomer concentration with the ethanol percentages of 10% (v/v) (a), 20% (v/v) (b) and 30% (v/v) (c)……...	69
Figure A11	Scanning electron micrographs of **PTES24C** spheres prepared under 3% NH_4OH catalytic process at 0.02 g/ml monomer concentration with the ethanol percentages of 10% (v/v) (a), 20% (v/v) (b) and 30% (v/v) (c)……...	69

Page

Figure A12 Scanning electron micrographs of **PTES24C** spheres prepared under 5% NH_4OH catalytic process at 0.02 g/ml monomer concentration with the ethanol percentages of 10% (v/v) (a), 20% (v/v) (b) and 30% (v/v) (c)……... 69

List of Schemes

		Page
Scheme 2.1	Synthetic pathway of 2,4-dimethoxycinnamic acid……	16
Scheme 2.2	Synthetic pathway of triethoxysilylpropyl-4-methoxy cinnamamide and triethoxysilylpropyl-2,4-dimethoxy cinnamamide……	18
Scheme 2.3	Synthetic pathway of polymerization reaction……..	20

List of Abbreviations

br	broad
^{o}C	degree Celsius
$CDCl_3$	deuterated chloroform
cm-1	unit of wavenumber (IR)
d	doublet (NMR)
DS	degree of substitution
FT-IR	Fourier transform infrared spectrophotometer
g	gram (s)
h	hour
IR	infrared
J	coupling constant
m	multiplet (NMR)
min	minute (s)
ml	milliliter (s)
mmol	millimole
mV	millivoltage
Mw	molecular weight
nm	nanometer (s)
NMR	nuclear magnetic resonance
PDI	polydispersity index
ppm	parts per million
s	singlet (NMR)
SEM	scanning electron microscopy
t	triplet (NMR)
TEM	transmission electron microscopy
UV	ultraviolet
v	volume

w	weight
δ	chemical shift
%	percent
λ	wavelength
µm	micrometer (s)

CHAPTER I

INTRODUCTION

Silsesquioxane

Hybrid inorganic–organic composites are new materials that hold significant promise. Nowadays, most of the hybrid materials that have already entered the market are synthesized and processed by using conventional soft chemistry based routes developed in the eighties. These groups of materials are being designed with the good physical and chemical properties associated with the inorganic part and the excellent choice of functional groups and chemical reactivity associated with organic part. Silicon-containing organic polymers in general and polysilsesquioxanes in particular have generated a great deal of interest because of their potential replacement and compatibility with silicon-based inorganic [1].

Silicon-network polymer was synthesized by hydrolytic condensation of a trialkoxysilane and having the general formula $(RSiO_{1.5})_n$ hence, they are known by the name silsesquioxanes. Silicon atom is bound to an average of one and a half oxygen atoms and to one hydrocarbon group. Typical functional groups that may be hydrolyzed and condensed include alkoxy- or chlorosilanes, silanols, and silanolates. Synthetic process that combine pH control of hydrolysis and condensation kinetics, surfactant-mediated polymer growth and molecular-templating mechanisms have been employed to control molecular–scale regularity [2-3].

The structures of the silsesquioxanes frameworks depend a great deal on the preparation method. They are uniquely sensitive to a highly interdependent combination of experimental factors including product solubilities, initial monomer concentration, nature and stability of the solvent, temperature, pH, the amount of free water available and the type of catalyst (acid or base) used to facilitate condensation.

Silsesquioxanes are depicted as bridging the property space between two component (inorganic–organic part) classes of materials. Many of these hybrid materials also exhibit an enhancement in properties such as thermal and thermo mechanical stability and solubility [4-6].

The initial discovery of these silsesquioxanes dates from 1946, when Scott [7] described completely condensed methyl-substituted silsesquioxanes. Since their discovery and isolation, many silsesquioxanes have been reported with synthetically useful functional groups.

Silsesquioxanes are most often prepared via hydrolytic condensation reactions of trifunctional organosilicon monomers, e.g., $RSiCl_3$ or $RSi(OMe)_3$.

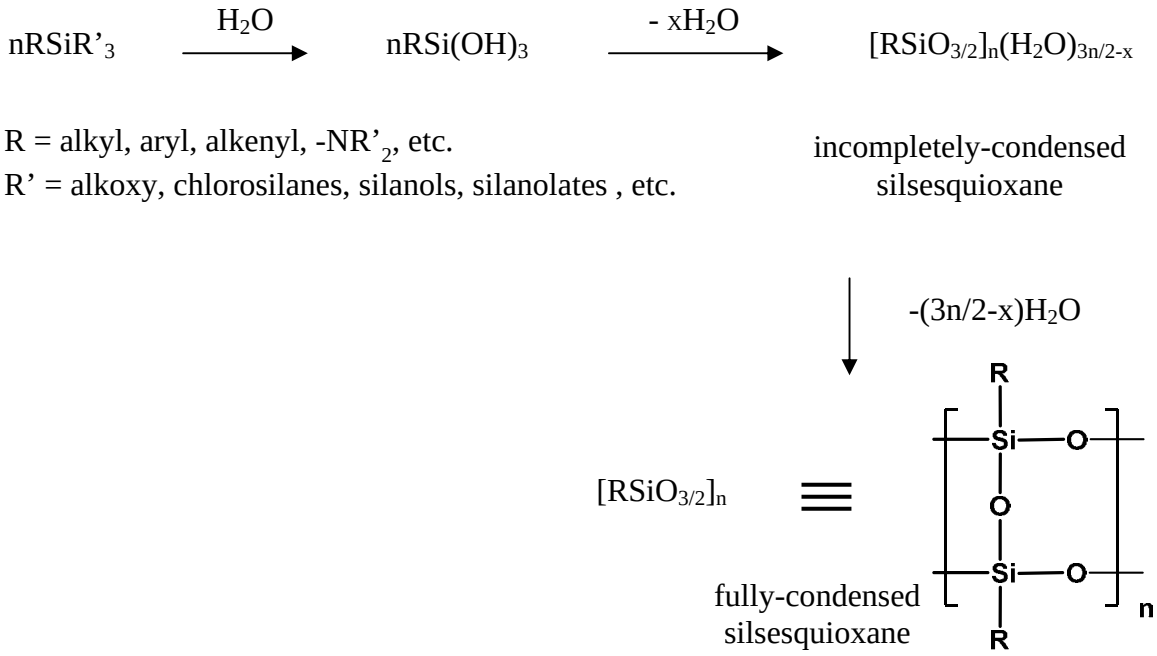

Figure 1.1 Hydrolytic condensation reactions of trifunctional organosilicon monomers [8].

Feher and co-workers [9] have extensively examined the chemistry of the vertex silicon atoms particularly the selective hydrolysis of one of the eight vertices in T8 cage (closed cubic) structures (Figure 1.2).

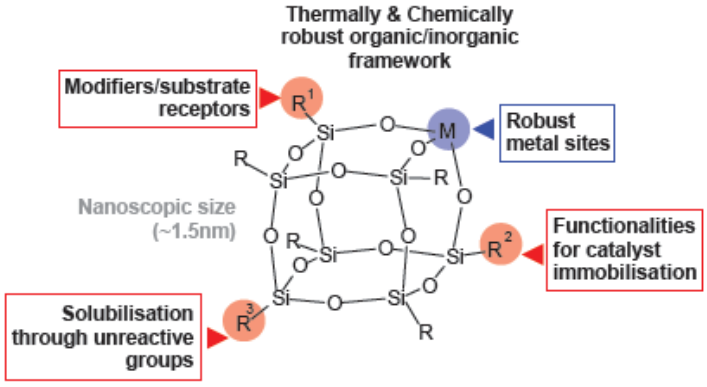

Figure 1.2 T8 cage (closed cubic) structures [10]

Lichtenhan Feher and Addenhuis were the pioneers in this particular subject of research and developed the preparation of completely and incompletely condensed silsesquioxanes on large scales at a short reaction time (Figure 1.3) [10].

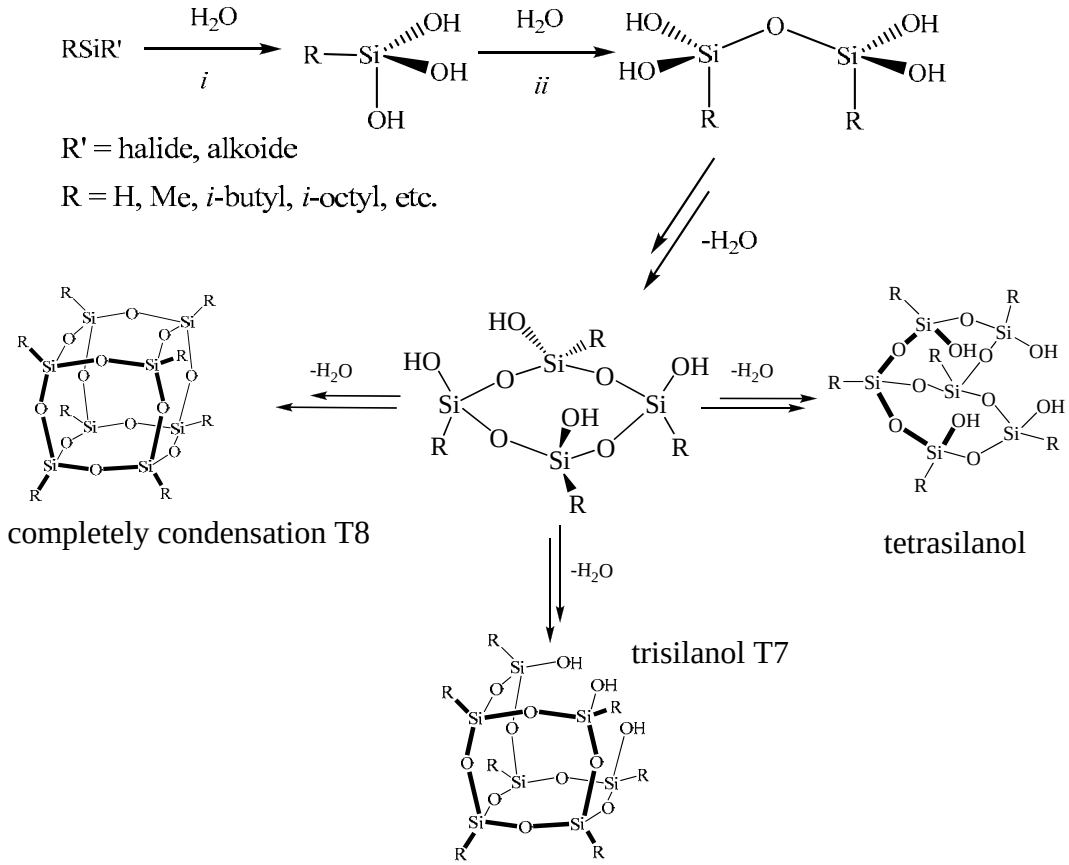

Figure 1.3 Synthesis of silsesqiuoxanes via polycondensation of trifunctional silanes [10].

3-Aminopropyltriethoxysilane

Molecular Formula: $C_9H_{23}NO_3Si$ Molecular Weight: 221

IUPAC Name: 1-Propanamine, 3-(triethoxysilyl)-

Synonyms: (3-Aminopropyl)triethoxysilane, APTES
3-(Triethoxysilyl)-1-propanamine
3-(Triethoxysilyl)propylamine
Propylamine
Silane 1100
Silane-(.gamma.-aminopropyl)triethoxy-
Silane-(3-aminopropyl)triethoxy-
Triethoxy(3-aminopropyl)silane, UC-A 1100)

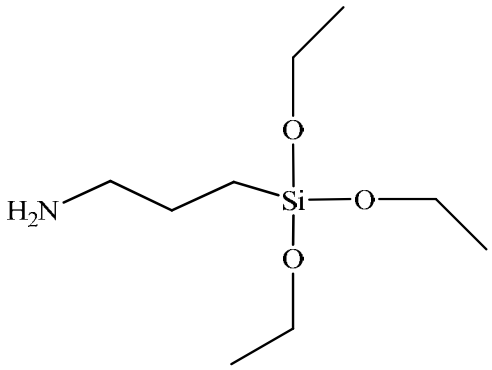

Figure 1.4 Structural Formula of 3-aminopropyltriethoxysilane [11]

The typical manufacturing procedure of 3-aminopropyltriethoxysilane (APTES) involves the catalyzed hydrogenation of the corresponding nitrile (2-cyanoethyltriethoxysilane) to produce the primary amino-functional silane. Vacuum distillation provides the highest quality version (Figure 1.5) [11].

Figure 1.5 Synthetic pathway of 3-aminopropyltriethoxysilane (APTES)

Physicochemical properties

The physical and chemical property data available for the APTES materials are in good agreement [11-12].

Table 1.1 Summary of physicochemical properties

Property	Value
Physical state	Liquid
Melting point	-70^{o}C
Boiling point	223^{o}C
Relative density	0.95 (25^{o}C)
Vapour pressure	0.02 hPa (20^{o}C)
Water solubility	7.6x105 mg/l (25^{o}C)

Stability in water and biodegradation

APTES is hydrolytically unstable ($t_{1/2}$ < 1 hour) over a range of environmentally relevant pH and temperature conditions (the data were presented in Table 1.2) [12].

Table 1.2 Summary of stability in water properties

pH	Half life (hours)		
	10 °C	24.7 °C	37 °C
4.7	0.97	0.41	0.22
7.0	56	8.4	3.9
9.0	0.78	0.15	0.043

The ethanol and trisilanols were produced rapid hydrolysis process. The Si-C bond will not further hydrolyze. That bond is hydrolytically stable and the aminopropyl group will not be cleaved. Only the ethoxy groups will be hydrolyzed. The transient silanol groups will condense with other silanols to yield:

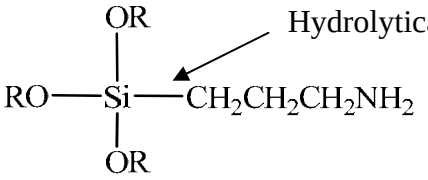

R = ether H or $SiCH_2CH_2CH_2NH_2(OR)_2$

Figure 1.6 Structure of hydrolytically stable bond from APTES

When water is added, a rapid hydrolysis of APTES proceeds to produce silanol. Hydrolysis of this material occurs rapidly and could be observed biodegradation of the hydrolysis products (silanols and ethoxy groups) [11-12].

APTES has been tested for acute toxicity by the oral, dermal, and inhalation routes of exposure in rats (the data were presented in Table 1.3).

Table 1.3 Summary of LD_{50} values

Tested	LD_{50}
Acute oral	1570 to 3650 mg/kg bw
Dermal	4.29 g/kg bw
Inhalation routes of exposure (saturated vapor of APTES)	Did not kill any of the 5 male or female rats (LT_{50} > 6 hours)

In this work, 4-methoxycinnamic acid and 2,4-dimethoxycinnamic acid were chosen as chromospheres, containing inside polysilsesquioxanes framework. This could be accomplished by linking the two chromophores, via amide bond, to the APTES amino group.

Cinnamic acid derivative

Esters of cinnamic acids and their close structural analogues have emerged as new sunscreens of the cinnamate class [13]. Esters of 4-methoxy cinnamic acid have been used widely in the cosmetic industry as stable UVB filter.

4-Methoxycinnamic acid exhibited a hepatoprotective activity in rat hepatocytes from toxicity induced by carbon tetrachloride (CCl_4). 4-Methoxy cinnamic acid had inhibitory effects on the diphenolase activity of mushroom tyrosinase and the inhibition was reversible [14]. Also, 4-methoxycinnamic acid showed the highest microbial α-glucosidase inhibitory activity [15].

2,4-Dimethoxycinnamic acid was firstly synthesized by Thitinun Monhaphol [16]. They showed excellent UV absorption ability and consider to be non-toxic and photostable compound.

In this work 4-methoxycinnamic acid and 2,4-dimethoxycinnamic acid were chosen as chromophores to condens with 3-aminopropyltriethoxysilane.

1.1 Literature reviews

In 1968, Stober and coworker synthesized spherical silica particles via a hydrolysis of alkyl silicates and subsequent condensation of silicic acid (tetraalkyl silicates) in different alcoholic solutions such as methanol, ethanol, n-propanol and n-butanol. Ammonia is used as a morphological catalyst. The particles' mean diameters were less than 0.05-2 μm (Figure1.7) [17].

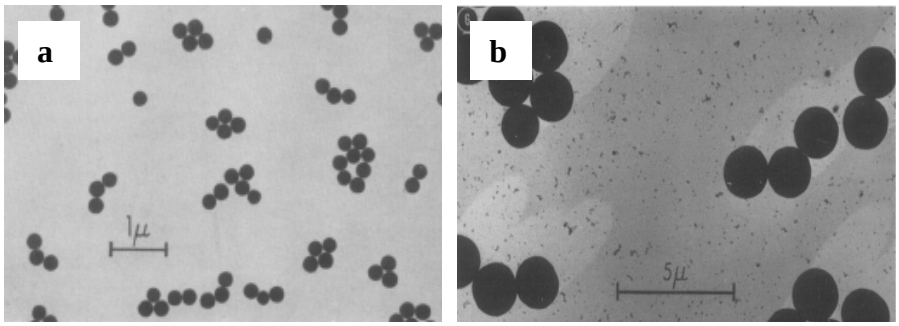

Figure 1.7 Electron micrograph of silica spheres obtained in the ethanol-ethyl ester system (a) and tetrapentyl silicate in a 3:1 propanol-methanol mixture (b) [17].

In 1998, Choi and coworker synthesized monodisperse, spherical organo-silica powders from an immiscible mixture of an aqueous NH_4OH solution and organo-alkoxysilanes such as phenyl-trimethoxysilane (PTMS), methyltrimethoxysilane (MTMS) and methyltriethoxysilane (MTES) (Figure 1.8). The organosilica powder was formed by the hydrolysis and condensation of the organo-alkoxysilane. The powders were obtained reproducibly under broad concentrations of organo alkoxysilanes 0.3–1.5 mol/L for PTMS, 0.3–0.6 mol/L for MTMS, and MTES, with concentrations of ammonia between 0.0625 and 2.0 mol/L [18].

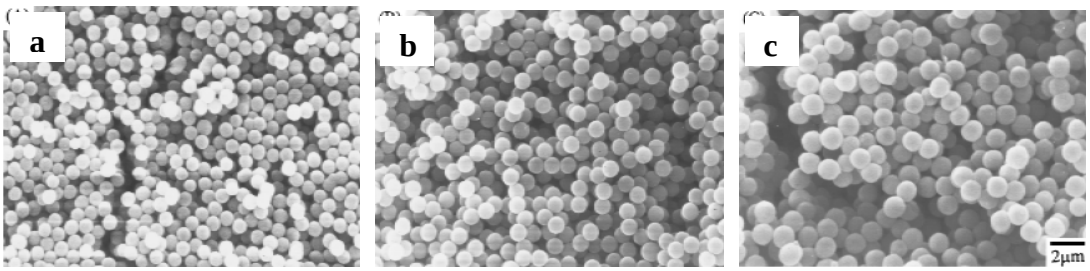

Figure 1.8 Scanning electron micrograph of organo-silica powders which are prepared PTMS(a), MTMS(b) and MTES(c). The concentrations of organo-alkoxysilanes and ammonia are 0.6 and 1.0 mol/L, respectively [18].

In 2000, Ottenbrite and coworker utilized 3-aminopropyltriethoxysilane (APTES) as the catalyst in the production of hybrid organo-silica nanoparticles from vinyltrimethoxysilane (VTS). Particles with size ranging from 100-500 nm could be prepared using organo-silanes in a water/surfactant solution (Figure 1.9 (a)). Based on elemental analysis, up to 10 mol% of APTES was incorporated into the siloxane particle network. It was demonstrated that the concentration of surfactant and APTES both affected the final particle size and stability against aggregation (Figure 1.9 (b)). This study showed that the APTES was effectively used as a self-catalyst and comonomer in the preparation of organosilica hybrid nanoparticles [19].

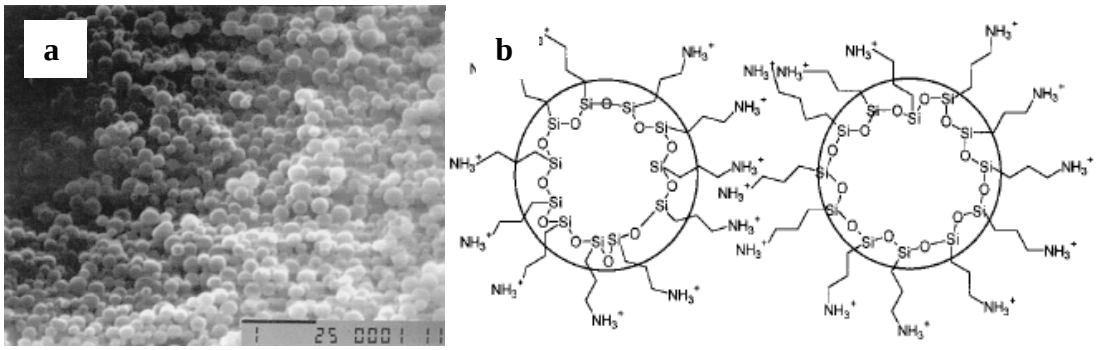

Figure 1.9 Scanning electron micrograph of particles obtained from VTS and comonomer (APTES) (a). Proposed steric and charge stabilization by APTES (b) [19].

In 2003, Lapidot and coworker loaded alone or as mixtures of several sunscreens, e.g. octyl methoxycinnamate (OMC), benzophenone-3 (BP-3), butyl methoxy dibenzoyl methane (BMDBM) and methyl benzylidene camphor (MBC) into the tetraethoxysilane (TEOS) microcapsules by interfacial polymerization process. The sizes of microcapsules were between 0.3–3 μm (Figure 1.10) [20].

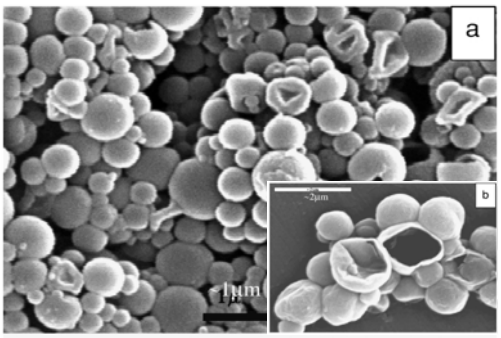

Figure 1.10 Scanning electron micrograph of OMC containing microcapsules and a rare open microcapsule [20].

In 2005, Kim and coworker prepared polysilsesquioxane spherical particle containing UVB filter from organotrialkoxysilane and cinnamic acid derivatives (Figure 1.11). This study showed that the polysilsesquioxane spherical particle possessed good physical properties and good UV-absorbing efficiency [21].

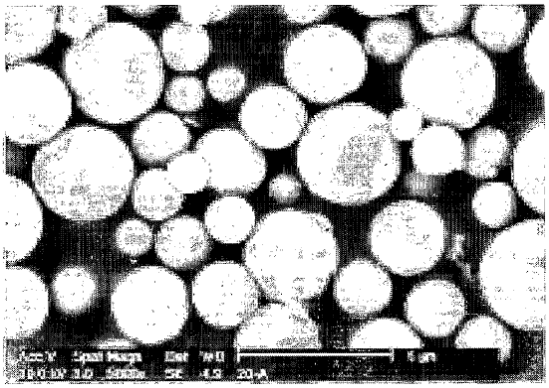

Figure 1.11 Scanning electron micrograph of polysilsesquioxane spherical particle containing UVB filter [21].

In 2006, Zhou and coworker synthesized hybrid organic-inorganic nanoballs block copolymers from 3-(trimethoxysilyl)propyl methacrylate (TMSPMA) and stearyl methacrylate (SMA) (Figure 1.12) through the initiation of chloro acetylferrocene using atom transfer radical polymerization (ATRP) in anisole solution. These resultant hybrid nanomaterials might become important in the new opportunities for applications in the field of electrochemical sensors and microcapsules [22].

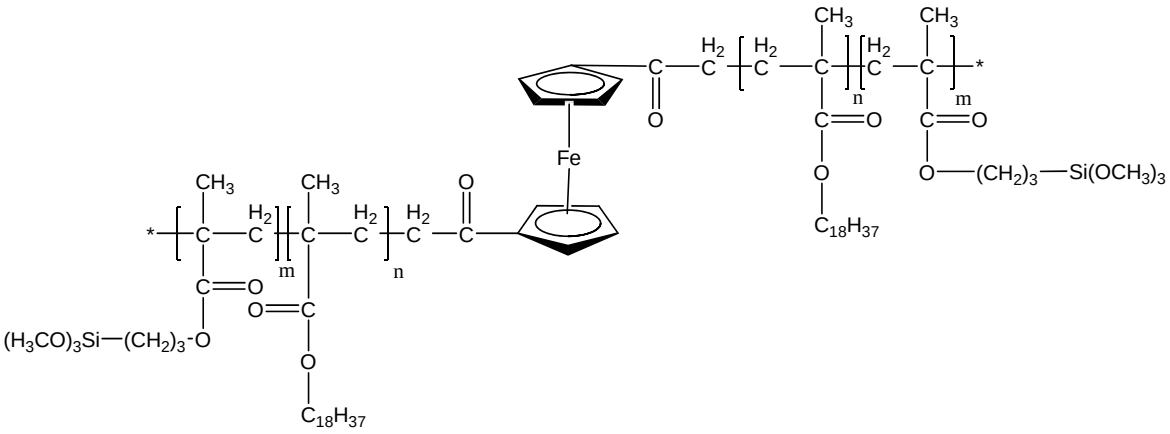

Figure 1.12 Structure of hybrid organic-inorganic nanoballs blockcopolymers [22]

In 2007, Khiterer and coworker synthesized 1,1'-bis[3-(trimethoxysilyl) propyl]-4,4'-bipyridiniumiodide and N,N'-bis[(3-trimethoxysilyl)propyl]ethylene diamine bridged polysilsesquioxane spherical (Figure 1.13) by inverse water-in-oil polymerization methods. Both are polycationic and can be used as carriers for polyanions such as DNA and construction of layer-by-layer architectures [23].

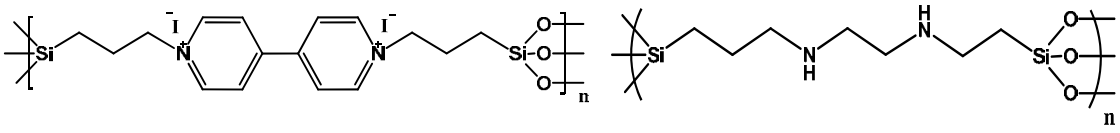

Figure 1.13 Structure of 1,1'-bis[3-(trimethoxysilyl)propyl]-4,4'-bipyridinium Iodide bridged polysilsesquioxane (left) and N,N'-bis[(3-trimethoxysilyl) propyl]ethylenediamine bridged polysilsesquioxane (right) [23].

In 2007, Martin and coworker coated chitosan films containing 86.4% deacetylated chitosan, 3-aminopropyltriethoxysilane (APTES) and gluteraldehyde on to an implant-quality titanium (Figure 1.14). The chitosan films were bound through a three-step process that involved the deposition of 3-amino propyltriethoxysilane (APTES) in toluene, followed by a reaction between the amine end of APTES with gluteraldehyde, and finally, a reaction between the aldehyde end of gluteraldehyde and chitosan. These materials can be found in the application of a bioactive coating on medical implant materials in orthopaedic and dental/craniofacial biomaterials [24].

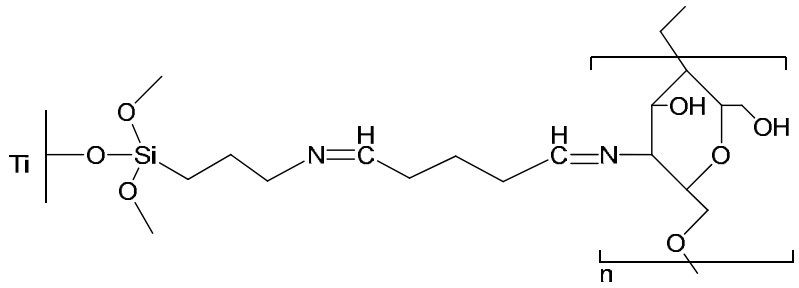

Figure 1.14 Structure of modified chitosan films [24]

In 2008, Ahn and coworker have demonstrated one-pot preparation of spherical silica microcapsules containing hydrophilic active compounds such as acetylsalicylic acid, 2,2′,4,4′-tetrahydroxybenzophenone (THBP) and synthetic dye (U1-Red) using a water-in-oil microemulsion process from the modified silicon alkoxides with 3-aminopropyltriethoxysilane (APTES) as a gelling agent. The properties of the microcapsules such as average particle size of 1–50 μm (Figure 1.15) and pore size distribution of 20–100 Å, were simply controllable by adjusting the characteristics of the precursors and the processing parameters. Spherical microcapsules were formed in the range of H_2O/Tetraethyl orthosilicate (TEOS) =1.5–1.7. The release rate rates of the encapsulated compounds were decreased with increasing the $H_2O$to-TEOS molar ratio due to the decrease of pore size in the denser structure of the microcapsules [25].

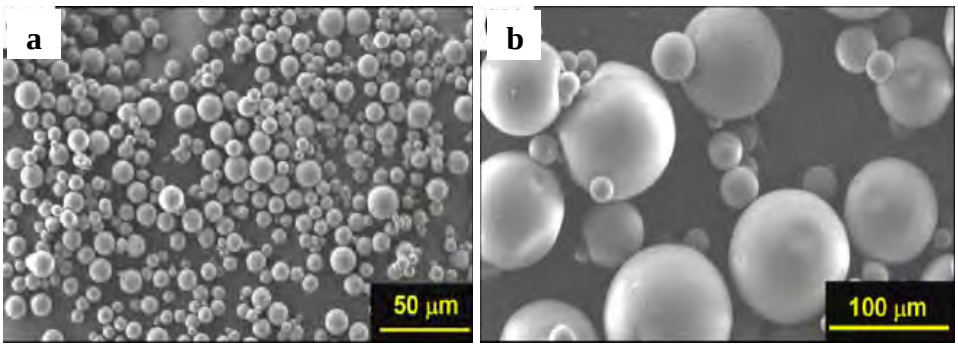

Figure 1.15 Scanning electron microscope images of the silica microcapsules formed at an impeller speed of 1,200 (a). The encapsulation precursor prepared in H_2O/TEOS=1.7. THBP was used as the hydrophilic active compound (b) [25].

In 2009, Lee and coworker synthesized polymer composite particles loaded with sunscreen agent, e.g. avobenzone (BMDBM), octyl salicylate and 2-ethylhexyl-4-methoxycinnamate (EHMC) from poly(methyl methacrylate) using a water-in-oil process (Figure 1.16). The particle sizes ranged between 0.01–1,000 µm and were stable at pH of 1.0-14.0 [26].

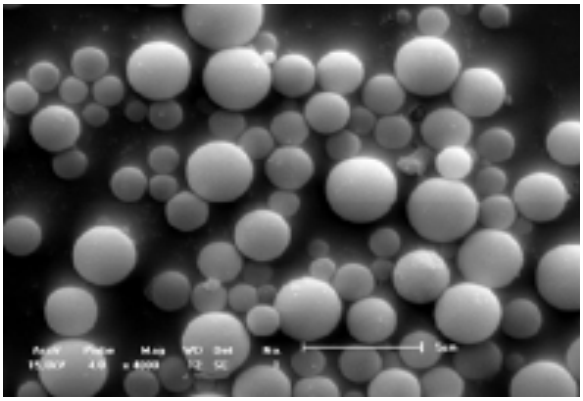

Figure 1.16 Scanning electron microscope images of particles from poly(methyl methacrylate) containing BMDBMA and 2-ethylhexyl 4-methoxycinnamate [26].

1.2 Research goal

The objectives of this research can be summarized as follows:

1. To synthesize polysilsesquioxane nanospheres containing two types of *trans*-substituted cinnamic acid derivatives, 4-methoxycinnamic acid and 2,4-dimethoxycinnamic acid.

2. To encapsulate 2-ethylhexyl-4-methoxycinnamate into the above spheres.

CHAPTER II

EXPERIMENTAL

2.1 Materials and Chemicals

3-Aminopropyltriethoxysilane (APTES), 4-methoxycinnamic acid and 2,4-dimethoxy benzaldehyde were purchased from Acros Organics (New Jersey, USA). 2-Ethylhexyl -4-methoxycinnamate (EHMC, Eusolex 2292) was obtained from Merck (Darmstadt, Germany). Pyridine and triethylamine (TEA) were purchased from J.T. Baker Inc. (New Jersey, USA). Piperidine was purchased from Aldrich Chemical Company (Steinheim, Germany). Toluene was purchased from Labscan (Dublin, Ireland). Ethanol was purchased from Merck (Damstadt, Germany). Calcium hydride was purchased from Fluka Chemical Company (Buchs, Switzerland). Calcium chloride and malonic acid were purchased from Carlo Erba Reagent (Milan, Italy). Thionyl chloride was obtained from the Department of chemistry, Faculty of science, Chulalongkorn University (old stock) and it was doubling distillated before use.

2.2 Instruments and Equipments

FT-IR analysis was carried out using a Nicolet Fourier transform Infrared spectrophotometer: Impact 410 (Nicolet Instruments Technologies, Inc., Madison, WI, USA). ^{1}H- and ^{13}C-NMR analyses were carried out using a Varian Mercury spectrometer which operated at 400.00 MHz for ^{1}H and 100.00 MHz for ^{13}C nuclei (Varian Company, Palo Alto, CA, USA). UV analysis was done with the aid of UV 2500 UV-Vis spectrophotometer (Shimadzu Corporation, Kyoto, Japan), using a quartz cell with 1 cm pathlength. Thin layer chromatography (TLC) was performed on aluminum sheets precoated with silica gel (Meck Kieselgel 60 F_{254}) (Merck KgaA, Darmstadt, Germany). Transmission Electron Microscopy (TEM) was carried out using JEM-2100 (Jeol, Ltd., Japan) and Scanning Electron Microscopy (SEM) was performed on JEM-6400 (Jeol, Ltd., Japan). The particle size was performed without prefiltering by Zetasizer nanoseries (Mulvern Instruments, Worcestershire, UK). SPF Analyzer (Optometrics, SPF-290s, MA, USA) was used as an apparatus for measuring the solar protection factor (SPF) and UV-A protection factor (UV-A PF)

2.3 Synthesis of 2,4-dimethoxycinnamic acids

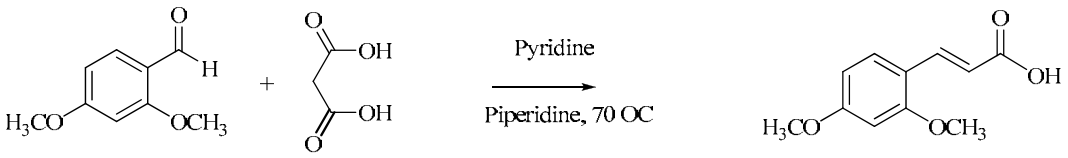

Scheme 2.1 Synthetic pathway of 2,4-dimethoxycinnamic acid.

2,4-Dimethoxycinnamic acid was synthesized using Knoevenagel-Doebner condensation [13] between benzaldehyde and malonic acid (Scheme 2.1). Briefly, 2,4-dimethoxy benzaldehyde (8.26 g, 0.05 mole) was dissolved in pyridine (48.3 ml, 0.6 mole). Then, malonic acid (5.2 g, 0.05 mole) and piperidine (2.47 ml, 25.25 mmole) were added. The reaction mixture was heated at 85 ^{O}C for 6-8 h. After the mixture had been cooled, cold 10% aqueous HCl were added. The solid was separated by suction filtration, washed with cold water and recrystallized with a mixture of water:ethanol (volume ratio 1:2). The 2,4-dimethoxycinnamic acids was characterized by NMR, IR spectroscopy (see in appendix **A1**).

2,4-Dimethoxycinnamic acid (**2,4-DMC**): light yellow solid. yield: 80.46%. FT-IR : 3465 (COO-H, stretching), 3003, 2937, and 2831 (H-C=C, stretching), 1671 (C=O, stretching) and 1592, 1449 and 791 (aromatic ring). ^{1}H-NMR (400 MHz, $CDCl_3$, δ, ppm): 10.55 (s, 1H, COOH), 7.76 (d, *J*=16.4 Hz, 1H, Ar-C**H**=), 7.59 (d, *J*=7.8 Hz, 1H, Ar-**H**), 6.68 (s, 1H, Ar-**H**), 6.57 (d, *J*=7.8 Hz, 1H, Ar**H**), 6.36 (d, *J*=16.4 Hz, 1H, =C**H**-COOH) and 3.85, 3.50 (s, 2x3H, 2xOC**H**$_3$).

2.4 Synthesis of hybrid monomers

Table 2.1 Condition used during the syntheses of hybrid monomers

Compound	Amounts of APTES	Cinnamic acid derivative	Amounts of *trans*-cinnamic acid
TES4C-1	22.13 g, 0.1 mol	4-methoxycinnamic acid **(4-MCA)**	17.81 g, 0.1 mol
TES4C-2			14.25 g, 0.08 mol
TES24C-1		2,4-dimethoxycinnamic acid **(2,4-DMC)**	20.82 g, 0.1 mol
TES24C-2			16.65 g, 0.08 mol

Triethoxysilylpropyl-4-methoxycinnamamide, **(TES4C)** and triethoxysilylpropyl-2,4-dimethoxy cinnamamide, **(TES24C)** could be done obtained from a condensation reaction between 3-aminopropyltriethoxysilane (APTES), 4-methoxycinnamoyl chloride and 2,4-dimethoxy cinnamoyl chloride, respectively (Scheme 2.2). **APTES** was reacted with two mole ratios of cinnamic acid derivative (see Table 2.1).

First, 4-methoxycinnamoyl chloride and 2,4-dimethoxycinnamoyl chloride were prepared by reacting 4-methoxycinnamic acid and 2,4-dimethoxycinnamic acid (see Table 2.1) with thionyl chloride (2.5-flod) in 200 ml of dry toluene. The mixture was refluxed for 6 h under N_2 atmosphere. Then, the solvent and excess thionyl chloride were removed by vacuum pump. Finally, toluene (5 ml) was added and removed the remaining of thionyl chloride.

Second, 4-methoxycinnamoyl chloride and 2,4-dimethoxycinnamoyl chloride were dissolved in 250 ml of dry toluene. Then, 3-aminopropyltriethoxysilane (APTES) (see Table 2.1) and triethylamine (TEA) (10.11 g, 0.1 mol) were added. The mixture was refluxed for 3 h under N_2 atmosphere. The solid salt of TEA - HCl was separated by suction filtration. The solvent and TEA were removed by rotary evaporation under reduced pressure. The obtained viscous liquid product was dried under vacuum to constant weight.

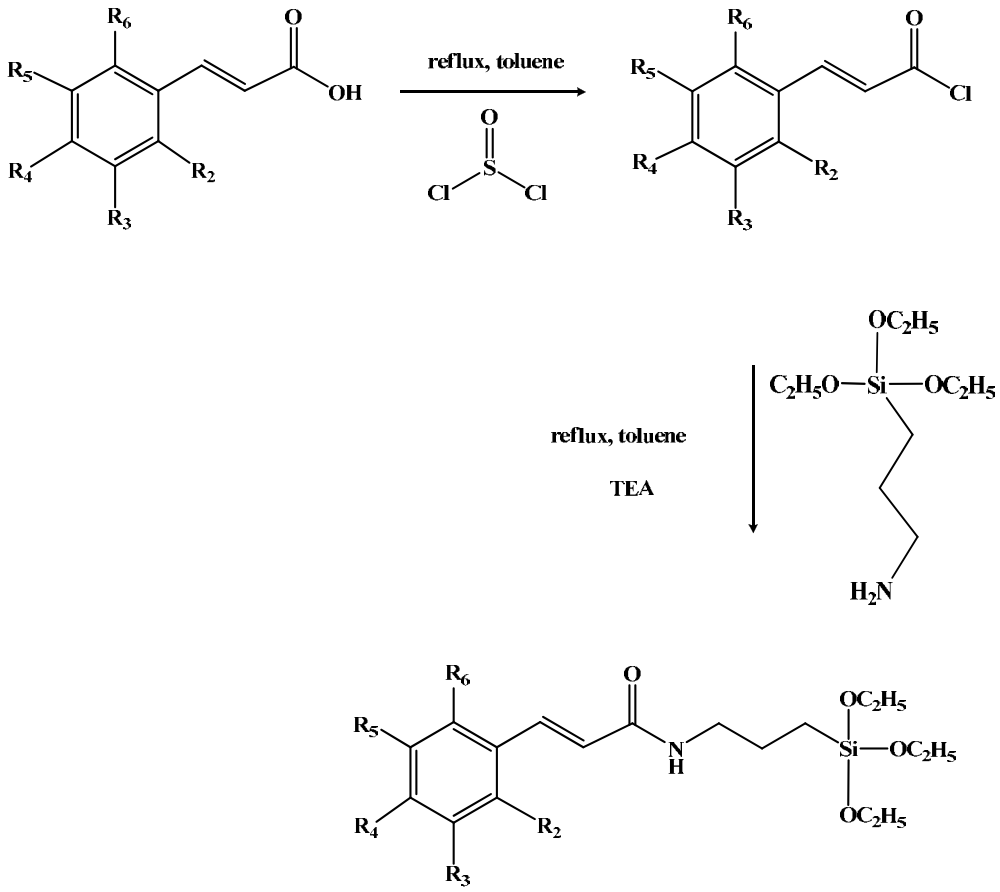

Scheme 2.2 Synthetic pathway of triethoxysilylpropyl-4-methoxycinnamamide and triethoxysilylpropyl-2,4-dimethoxycinnamamide

Compound	R_2	R_3	R_4	R_5	R_6
Triethoxysilylpropyl-4-methoxycinnamamide **(TES4C)**	H	H	OCH_3	H	H
Triethoxysilylpropyl-2,4-dimethoxycinnamamide **(TES24C)**	OCH_3	H	OCH_3	H	H

Triethoxysilylpropyl-4-methoxycinnamamide ***(TES4C-1)*** products

TES4C-1: red-brown oil. % conversion: 0.98. yield: 96.46%. FT-IR: 3276 (-NH, stretching), 2966 (-C-H, stretching), 1655 (C=O, stretching), 1602 (aromatic ring, stretching), 1545 (-NH, bending), 1509 (aromatic ring, stretching), 1061 (C-O, stretching) and 947 (aromatic ring, bending). ^{1}H-NMR (400 MHz, $CDCl_3$, δ, ppm): 7.56 (d, *J*=15.6 Hz, 1H, Ar-C**H**=), 7.42 (d, *J*=8.4 Hz, 1H, Ar-**H**), 6.88 (d, *J*=8.8 Hz, 1H, Ar-**H**), 6.24 (d, *J*=15.6 Hz, 1H, =C**H**-CONH), 5.91 (br, s, 1H, -CON**H**), 3.83 (m, 2H, -OC**H**$_2$-CH_3), 3.82 (s, 3H, -OC**H**$_3$), 3.38 (m, 2H, -NH-C**H**$_2$-CH_2-), 1.69 (m, 2H, -CH_2-C**H**$_2$-CH_2), 1.21 (m, 3H, -OCH_2-C**H**$_3$) and 0.68 (m, 2H, -CH_2-C**H**$_2$-Si-).

Triethoxysilylpropyl-4-methoxycinnamamide ***(TES4C-2)*** products

TES4C-2: red-brown oil. % conversion: 0.8. yield: 94.30%. FT-IR: 3277 (-NH, stretching), 2965 (-C-H, stretching), 1655 (C=O, stretching), 1604 (aromatic ring, stretching), 1547 (-NH, bending), 1508 (aromatic ring, stretching), 1069 (C-O, stretching) and 827 (aromatic ring, bending). ^{1}H-NMR (400 MHz, $CDCl_3$, δ, ppm): 7.56 (d, *J*=15.6 Hz, 1H, Ar-C**H**=), 7.43 (d, *J*=8.8 Hz, 1H, Ar-**H**), 6.87 (d, *J*=8.8 Hz, 1H, Ar-**H**), 6.24 (d, *J*=15.6 Hz, 1H, =C**H**-CONH), 5.96 (br, s, 1H, -CON**H**), 3.82 (m, 2H, -OC**H**$_2$-CH_3), 3.81 (s, 3H, -OC**H**$_3$), 3.37 (m, 2H, -NH-C**H**$_2$-CH_2-), 1.69 (m, 2H, -CH_2-C**H**$_2$-CH_2), 1.18 (m, 3H, -OCH_2-C**H**$_3$) and 0.67 (m, 2H, -CH_2-C**H**$_2$-Si-).

Triethoxysilylpropyl-2,4-dimethoxycinnamamide ***(TES24C-1)*** products

TES24C-1: yellow-brown oil. % conversion: 0.92. yield: 94.984%. FT-IR: 3259 (-NH, stretching), 2965 (-C-H, stretching), 1649 (C=O, stretching), 1601, (aromatic ring, stretching), 1562 (-NH, bending), 1502 (aromatic ring, stretching), 1079 (C-O, stretching) and 836 (aromatic ring, bending). ^{1}H-NMR (400 MHz, $CDCl_3$, δ, ppm): 7.74 (d, *J*=16 Hz, 1H, Ar-C**H**=), 7.38 (d, *J*=8.4 Hz, 1H, Ar-**H**), 6.47 (d, *J*=8.8 Hz, 1H, Ar-**H**) 6.44 (s, 1H, Ar-**H**), 6.41 (d, *J*=16.4 Hz, 1H, =C**H**-CONH), 5.86 (br, s, 1H, -CON**H**), 3.84, 3.82 (s, 2x3H, 2xOC**H**$_3$), 3.82 (m, 2H, -OC**H**$_2$-CH_3), 3.37 (m, 2H, -NH-C**H**$_2$-CH_2-), 1.68 (m, 2H, -CH_2-C**H**$_2$-CH_2), 1.22 (m, 3H, -OCH_2-C**H**$_3$) and 0.67 (m, 2H, -CH_2-C**H**$_2$-Si-).

Triethoxysilylpropyl-2,4-dimethoxycinnamamide ***(TES24C-2)*** products

TES24C-2: yellow-brown oil. % conversion: 0.78. yield: 92.99%. FT-IR: 3262 (-NH, stretching), 2967 (-C-H, stretching), 1642 (C=O, stretching), 1608, (aromatic ring, stretching), 1555 (-NH, bending), 1499 (aromatic ring, stretching), 1074 (C-O, stretching) and 838 (aromatic ring, bending). ^{1}H-NMR (400 MHz, $CDCl_3$, δ, ppm): 7.74 (d, *J*=16 Hz, 1H, Ar-C**H**=), 7.37 (d, *J*=8 Hz, 1H, Ar-**H**), 6.46 (d, *J*=8 Hz, 1H, Ar-**H**) 6.43 (s, 1H, Ar-**H**), 6.41 (d, *J*=16 Hz, 1H, =C**H**-CONH), 5.93 (br, s, 1H, -CON**H**), 3.83, 3.81 (s, 2x3H, 2xOC**H**$_3$), 3.82 (m, 2H, -OC**H**$_2$-CH_3), 3.37 (m, 2H, -NH-C**H**$_2$-CH_2-), 1.68 (m, 2H, -CH_2-C**H**$_2$-CH_2), 1.21 (m, 3H, -OCH_2-C**H**$_3$) and 0.67 (m, 2H, -CH_2-C**H**$_2$-Si-).

2.5 Micro/nanoparticles formation

Micro/nanoparticles were prepared simultaneously during the polymerization reaction (Scheme 2.3). The formations of particles from both hybrid monomers at room temperature using ethanol as a solvent through self-catalysis, acid-catalysis and basic-catalysis were compared (see Table 2.2- Table2.3).

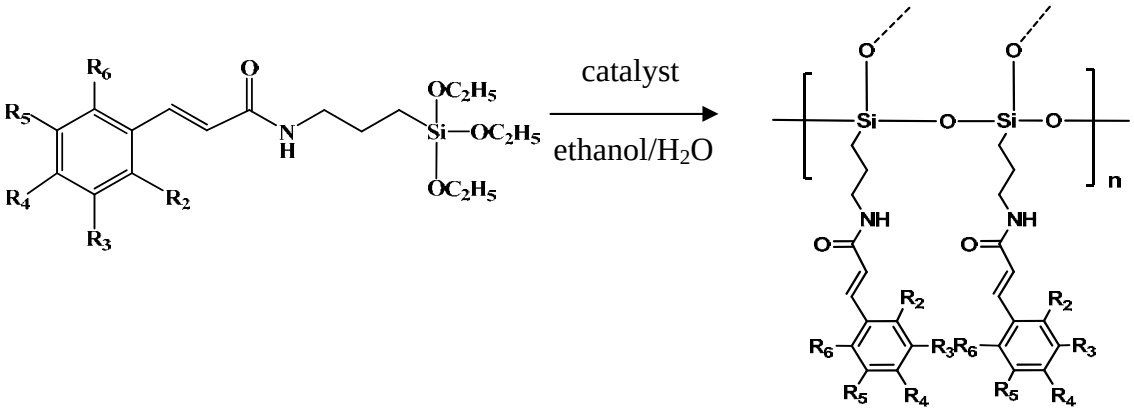

Scheme 2.3 Synthetic pathway of polymerization reaction

2.5.1 Poly[propyl-4-methoxycinnamamidesilsesquioxane] (PTES4C) products

Acid and basic catalyst process (external catalysts) [4, 17]

The hybrid monomer **TES4C-1** was dissolved in various volume of ethanol, i.e. 4, 6, 8 ml. The obtained clear solution was dropped slowly and stirred simultaneously into the water phase, i.e. 16, 14, 12 ml, respectively in a presence of catalyst (0.1% HCl, 3% NH_4OH or 5% NH_4OH).

Then, the obtained suspension was stirred for 24 h at room temperature (see Figure 2.1 and Table 2.2 for condition used during synthesized **TES4C-1**).

Self-catalysis process (internal catalysts) [19]

The hybrid monomer **TES4C-2** was dissolved in various volume of ethanol, i.e. 2, 4, 6, 8 ml. The obtained clear solution was dropped slowly and stirred simultaneously into the water phase, i.e. 18, 16, 14, 12 ml, respectively.

Then, the obtained suspension was stirred for 24 h at room temperature (see Figure 2.1 and Table 2.2 for condition used during synthesized **TES4C-2**).

TES4C	Catalysts/ water phase
TES4C-1	0.1% HCl
	3% NH_4OH
	5% NH_4OH
TES4C-2	distilled H_2O (self-catalysis)

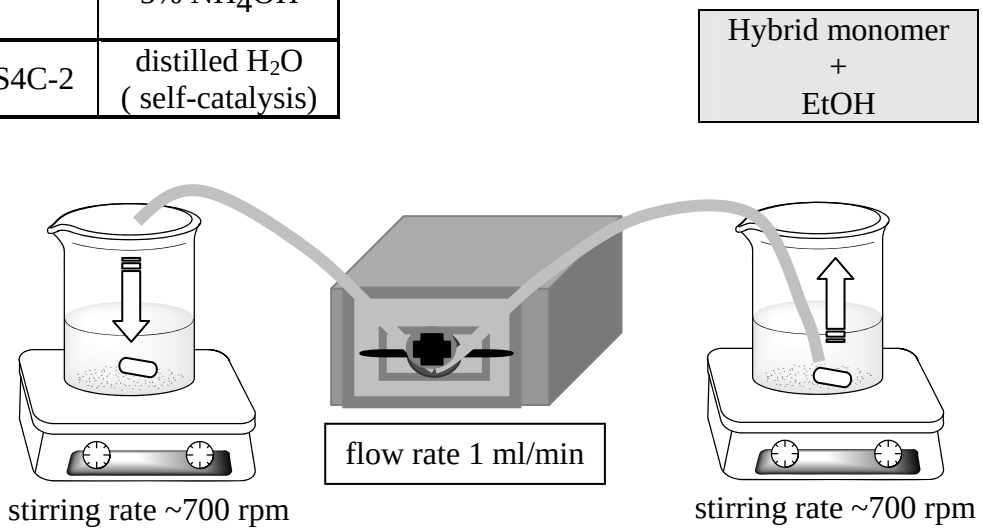

Figure 2.1 Particles formation processes of **TES4C**

2.5.2 Poly[propyl-2,4-dimethoxycinnamamidesilsesquioxane] (PTES24C) products

Acid and basic catalyst process (external catalysts) [4, 17]

The hybrid monomer **TES24C-1** was dissolved in various volume of ethanol, i.e. 2, 4, 6 ml. The obtained clear solution, the water phase (i.e. 18, 16, 14 ml, respectively) in a presence of catalyst (0.1% HCl, 3% NH_4OH or 5% NH_4OH) was dropped slowly and stirred simultaneously into clear solution.

Then, the obtained suspension was stirred for 24 h at room temperature (see Figure 2.2 and Table 2.3 for condition used during synthesized **TES24C-1**).

Self-catalysis process (internal catalysts) [19]

The hybrid monomer **TES24C-2** was dissolved in various volume of ethanol, i.e. 2, 4, 6 ml. The obtained clear solution, the distilled water (i.e. 18, 16, 14 ml, respectively) was dropped slowly and stirred simultaneously into clear solution.

Then, the obtained suspension was stirred for 24 h at room temperature (see Figure 2.2 and Table 2.3 for condition used during synthesized **TES24C-2**).

TES24C	Catalysts/ water phase
TES24C-1	0.1% HCl
	3% NH_4OH
	5% NH_4OH
TES24C-2	distilled H_2O (self-catalysis)

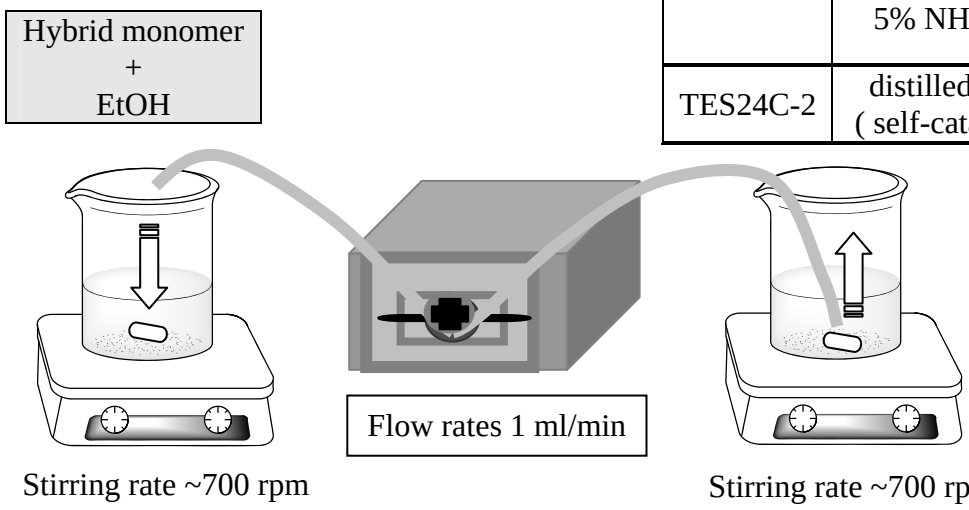

Figure 2.2 Particles formation processes of **TES24C**

Table 2.2 Condition used during the synthesized poly[propyl-4-methoxycinnamamide silsesquioxane] **(PTES4C)** nanospheres

Catalyst	TES4C	Concentration of monomer (g/ml)	% EtOH (v/v)
0.1% HCl	0.40 g, 0.001 mol	0.02	20
		0.02	30
		0.02	40
3% NH_4OH		0.02	20
		0.02	30
		0.02	40
5% NH_4OH		0.02	20
		0.02	30
		0.02	40
Self-catalysis	0.40 g, 0.001 mol	0.02	10
		0.02	20
		0.02	30
		0.02	40
	0.80 g, 0.002 mol	0.04	20
	1.20. g, 0.003 mol	0.06	20

Table 2.3 Condition used during the synthesized poly[propyl-2,4-dimethoxycinna-mamidesilsesquioxane] **(PTE24C)** nanospheres

Catalyst	TES4C	Concentration of monomer (g/ml)	% EtOH (v/v)
0.1% HCl	0.41 g, 0.001 mol	0.02	10
		0.02	20
		0.02	30
3% NH_4OH		0.02	10
		0.02	20
		0.02	30
5% NH_4OH		0.02	10
		0.02	20
		0.02	30
Self-catalysis	0.40 g, 0.001 mol	0.02	10
		0.02	20
		0.02	30
	0.82 g, 0.002 mol	0.04	20
	1.23 g, 0.003 mol	0.06	20

Then, the obtained **PTES4C** and **PTES24C** suspension products were washed to remove the last trace of monomer by dialysis method (20% ethanol) and stirred for 24 h at room. The obtained solid product was dried under vacuum to constant weight and the synthesis yield was evaluated.

Afterward, the particles were subjected to redispersibility after dissolved in distilled water. The colloidal stability and aggregation behavior of the aqueous suspensions were observed by vision at room temperature within 1 week.

2.6 Effect of surfactant [21, 25]

The study effect of added surfactant during polymerization processes, 0.40 g, 0.001 mol of **TES4C** (or 0.41 g, 0.001 mol of **TES24C**) was dissolved in 1 ml of Triton X-100 (without using ethanol as a solvent). The process was carried out in the same method as micro/nanoparticles formation through self-catalysis process (see Section 2.5.1 and 2.5.2). Then, the obtained suspension products were washed to remove the last trace of monomer and surfactant by dialysis method (20% ethanol) and stirred for 24 h at room. The obtained solid product was dried under vacuum to constant weight and the synthesis yield was evaluated.

2.7 Encapsulation process [20, 25]

The 2-ethylhexyl-4-methoxycinnamate (**EHMC**) was chosen as a model compound for encapsulation.

EHMC-encapsulated **PTES4C** was prepared from mixture of 0.20 g, 0.0007 mol **EHMC** and 0.40 g, 0.001 mol of **TES4C** in ethanol. The obtained clear solution was dropped slowly (1 ml/min) and stirred simultaneously (stirring rate ~700 rpm) into water phase. Then, the obtained suspension was stirred for 24 h at room temperature

EHMC-encapsulated **PTES24C** was prepared from mixture of 0.20 g, 0.0007 mol **EHMC** and 0.41 g, 0.001 mol of **TES24C** dissolved in 1 ml of Triton X-100 (without using ethanol as a solvent). The obtained clear solution, distilled water was dropped slowly (1 ml/min) and stirred simultaneously (stirring rate ~700 rpm) into water phase. Then, the obtained suspension was stirred for 24 h at room temperature.

Then, the particle suspension was centrifuged and redispersed in water, subjected to optimized % encapsulation efficiency and % loading capacity. The extracted concentration of **EHMC** was recovered in the partition between hexane/water phase and in the hexane phase was determined using UV absorption spectroscopy with the aid of a calibration curve (Appendix **B**).

2.8 Particle size, SEM and TEM analyses

The average particle size was measured by Mastersizer S (Mulvern Instruments, Worcestershire, UK) equipped with a He-Ne laser beam at 632.8 nm (scattering angle of 173º) at 25 ± 2ºC. Each measurement was repeated five times and an average value was reported**.**

Mean diameter of the resulted spherical particles was determined from an image of a scanning electron microscope (SEM; JEM-6400, JEOL, Japan). A drop of the nanoparticle suspension was placed on a glass slide and dried. The sample was coated with a gold layer under vacuum at 15 kV for 90 s. The coated sample was then mounted on an SEM stud for visualization. Analysis was carried out at 25 ± 2ºC. Diameters of 100 spherical shown in a scanning electron microscope photographs were calculated to estimate their mean as mean diameter.

TEM photographs were acquired on a transmission electron microscope (JEM-2100, JEOL, Japan). A drop of nanoparticles suspension was placed on a carbon film coated on a copper grid and dried. Observation was performed at 100-120 kV.

CHAPTER III

RESULT AND DISCUSSION

3.1 Hybrid monomers

In this research, polysilsesquioxane micro/nanospherses with UV absorption property were prepared. Two chromosphores, *tran*-4-methoxycinnamic acid (UV-B absorptive chromosphore) and *tran*-2,4-dimethoxycinnamic acid (UV-A absorptive chromosphore) were integrated into the monomeric structure.

The synthesized 2 groups of hybrid monomer compounds were successfully synthesized using condensation reaction between 3-aminopropyltriethoxy silane **(APTES)** and *trans*-4-methoxycinnamic acid and *trans*-2,4-dimethoxycinnamic acid, respectively. The obtained triethoxysilylpropyl-4-methoxycinnamamide, (**TES4C**, a UV-B absorptive chromosphore) and triethoxysilylpropyl-2,4-dimethoxycinnamamide, (**TES24C**, a UV-A absorptive chromosphore). These two synthesized hybrid monomers were both prepared at two conversion percentages, the hybrid monomer with and without residues of free amine. Structures of the products were elucidated using ^{1}H-NMR, IR and UV absorption.

3.1.1 Synthesis of triethoxysilylpropyl-4-methoxycinnamamide (TES4C) hybrid monomers

The ^{1}H-NMR spectra of **APTES** in $CDCl_3$ shows resonances of the methylene proton (NH_2-C**H**$_2$-) at approximately 2.6 ppm (Appendix **A2**) while the ^{1}H-NMR spectrum of the synthesized **TES4C** showed resonances of the methylene proton (-CONH-C**H**$_2$-) at 3.3 ppm, **(b)** and amide protons at 5.9 ppm, **(f)**. The *trans*-configuration of C=C of 4-methoxycinnamoyl moiety was confirmed through the appearance of the two signals at approximately 7.56 ppm, **(g')** and 6.24 ppm, (**g**) with J = 15.6 Hz (Figure 3.1).

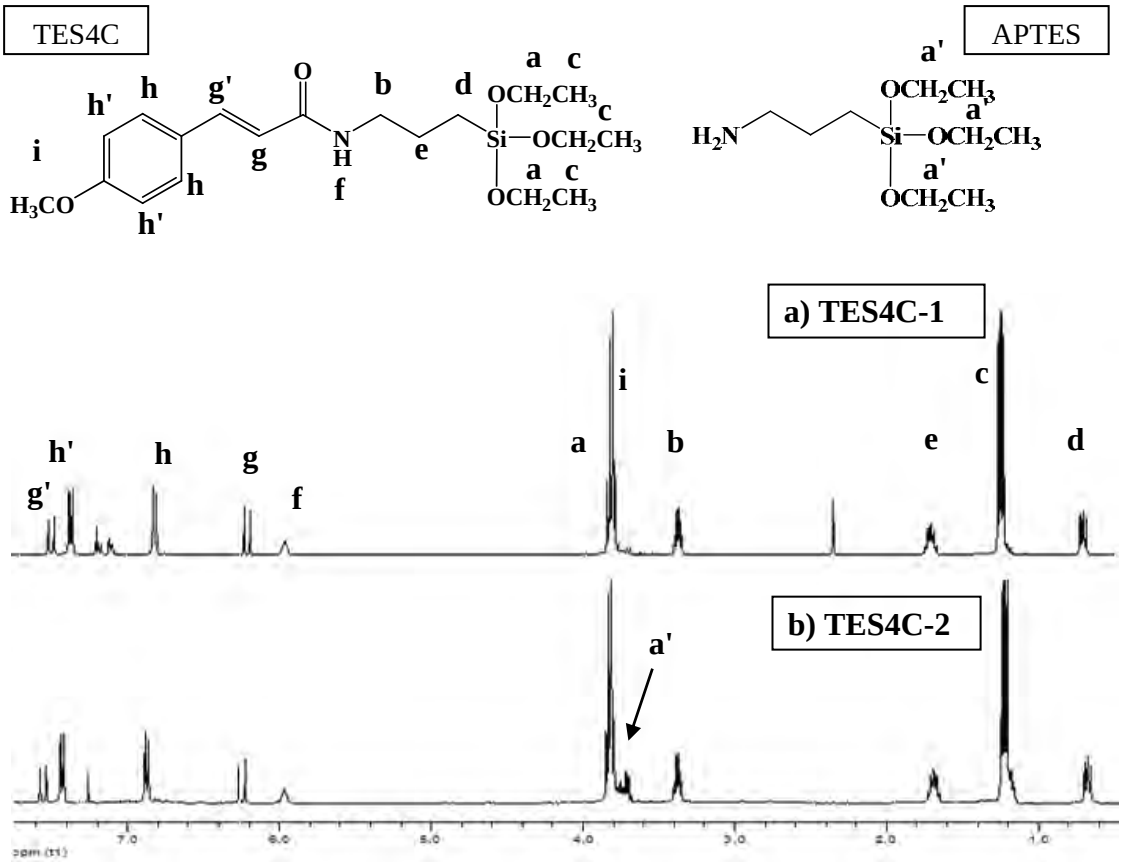

Figure 3.1 ^{1}H-NMR spectrum and structure of triethoxysilylpropyl-4-methoxy cinnamamide, (**TES4C-1**, (a) and **TES4C-2**, (b)) in $CDCl_3$.

Amount of **TES4C** generated (compared to **APTES**) was deduced from the ^{1}H-NMR spectrum of each product using the integration of peaks at 7.56 ppm (Ar-C**H**=) and 0.67 ppm (-CH_2-C**H**$_2$-Si-), (Figure 3.4). It was found that the **TES4C-1** product has residue of 2% **APTES** while the **TES4C-2** product has residue of 20% APTES.

The ^{1}H-NMR spectra of **TES4C-1** and **TES4C-2** in $CDCl_3$ were similar except that only **TES4C-2** showed peak at 3.7 (**a'**, **APTES**, -OC**H**$_2$-CH_3). The peaks at 3.7 ppm of APTES (-OCH2-CH3) and at 3.37 ppm (-CO-NH-CH2-CH2-) of TES4C-2 were compared and % conversion could be deduced.

The structure of the two **TES4C** hybrid monomers was also confirmed by FT-IR and UV-vis spectroscopy. The FT-IR spectrum of 4-methoxycinnamic acid (Figure 3.2, (b)) showed C=O stretching at approximately 1670 cm^{-1} (carboxyl group of carboxylic functionality) while that of **TES4C** showed C=O stretching of amide group at 1655 cm^{-1}. In addition, the spectrum of the product showed obvious -NH stretching and -NH bending absorption bands of amide group at approximately 3200 cm^{-1} and 1540 cm^{-1}, respectively. The C-H stretching of aromatic ring was shown at approximately 1600 cm^{-1} and the C-H bending of the aromatic ring could be observed at approximately 900 cm^{-1}. The absorption peaks of the C-O stretching could be observed at approximately 1060 cm^{-1}.

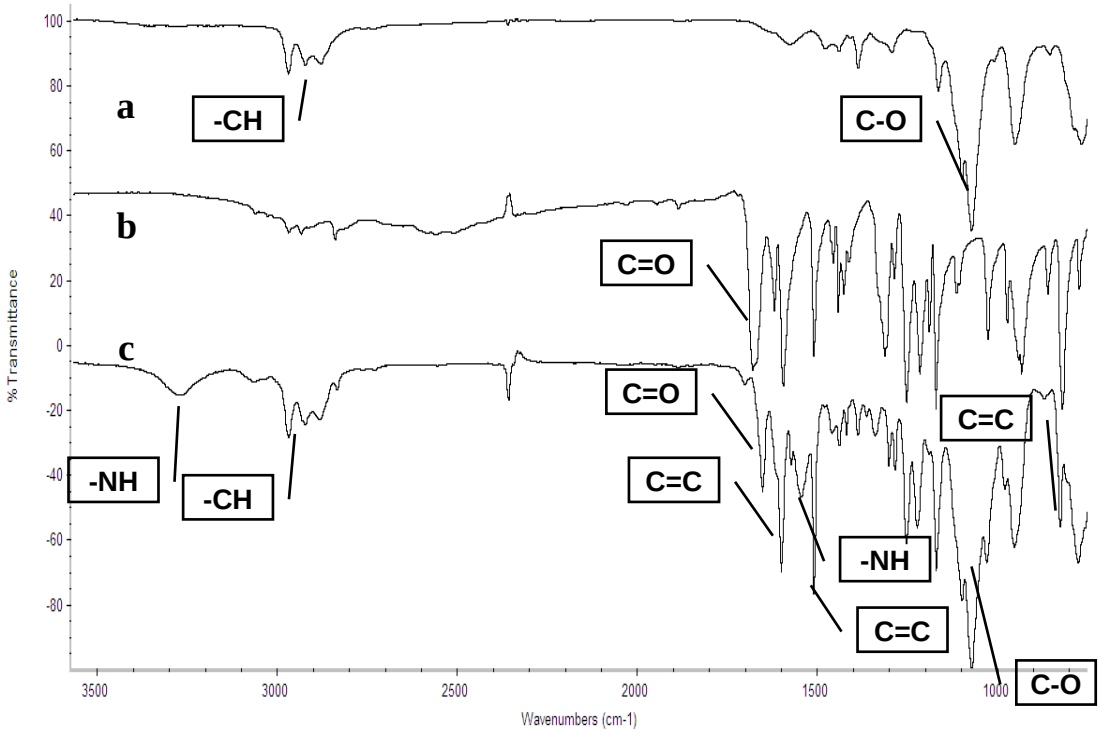

Figure 3.2 FT-IR spectra of 3-aminopropyltriethoxysilane **(APTES)** (a), 4-methoxycinnamic acid (b) and triethoxysilylpropyl-4-methoxycinnamamide, **(TES4C-1)** (c).

UV spectrum of **TES4C** showed obvious absorption in the UVB region (λ_{max} ~291 nm), (Figure 3.3). Thus, it could be concluded that 4-methoxycinnamic acid was successfully integrated into the monomeric structure.

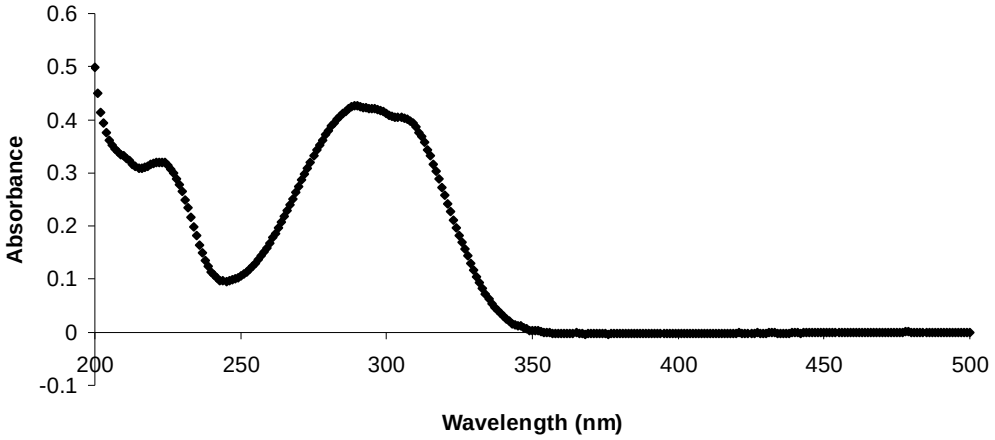

Figure 3.3 UV absorption spectrum of **TES4C-2** at molar absorptivity1.31 x 10^{-5} M.

3.1.2 Synthesis of triethoxysilylpropyl-2,4-dimethoxycinnamamide (TES24C) hybrid monomers

2,4-Dimethoxycinnamic acid was successfully synthesized using Knoevenagel-Doebner condensation between benzaldehyde and malonic acid. Its structure (see chapter II, Scheme 2.1) was characterized using ^{1}H-NMR, and FT-IR (Appendix **A1**). The *trans*-configuration of C=C of 2,4-dimethoxycinnamic acids was confirmed by ^{1}H-NMR; two signals at approximately 7.76 and 6.36 ppm with *J* of 16.4 Hz.

The ^{1}H-NMR spectra of **APTES** in $CDCl_3$ shows resonances of the methylene proton (NH_2-C**H**$_2$-) at approximately 2.6 ppm (Appendix **A2**) while the ^{1}H-NMR spectrum of the synthesized **TES24C** shows resonances of the methylene proton (-CONH-C**H**$_2$-) at 3.37 ppm, **(b)** and amide protons at approximately 5.9 ppm, **(f)**. The *trans*-configuration of C=C double bond of 2,4-methoxycinnamoyl substitution was confirmed through the appearance of the two signals at approximately 7.74 ppm, **(g')** and 6.41 ppm, **(g)** with *J* = 16 Hz (Figure 3.4).

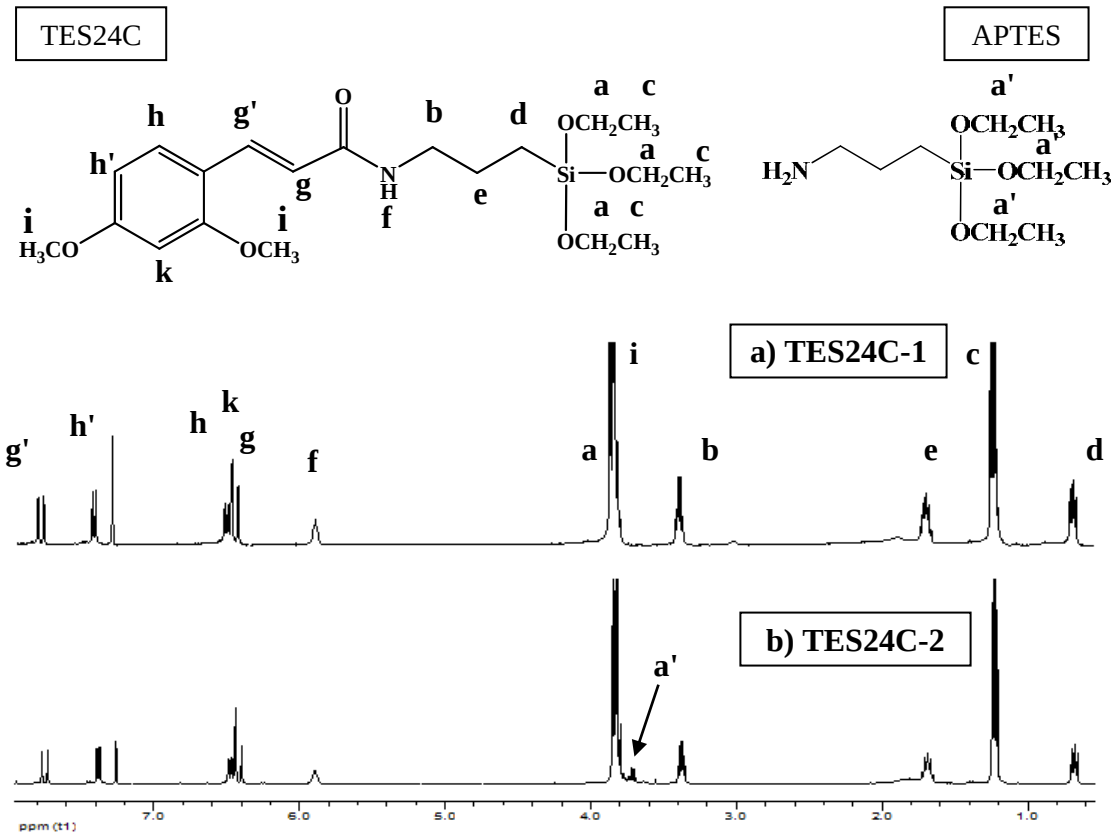

Figure 3.4 ^{1}H-NMR spectrum and structure of triethoxysilylpropyl-4-methoxy cinnamamide, (**TES24C-1**, (a) and **TES24C-2**, (b)) in $CDCl_3$.

Amount of **TES24C** generated (compared to **APTES**) was obtained from the ^{1}H-NMR spectrum of each product using the integration of peaks at 7.74 ppm (Ar-C**H**=) and 0.67 ppm (-CH_2-C**H**$_2$-Si-), (Figure 3.4). It was found that the **TES4C-1** product contained 8% **APTES** residue while the **TES4C-2** product contained 22% APTES residue.

The ^{1}H-NMR spectrum of **TES24C-1** and **TES24C-2** in $CDCl_3$ are similar except that the latter showed bigger signal at 3.7, (**a'**, **APTES**, -OC**H**$_2$-CH_3). The peaks between at 3.7 ppm of **APTES** (-OC**H**$_2$-CH_3) and at 3.37 ppm (-CO-NH-**CH**$_2$-CH_2-) of **TES24C-2** were compared and the result agreed well with the 22% of APTES in the product.

The structure of the two **TES24C** hybrid monomers was also confirmed by FT-IR and UV-vis spectroscopy. The FT-IR spectrum of 2,4-dimethoxycinnamic acid (Figure 3.5, (b)) showed C=O stretching at approximately 1670 cm^{-1} (carboxyl group of carboxylic functionality) while that of **TES24C** showed C=O stretching of amide group at approximately 1640 cm^{-1}. In addition, the spectrum of the product showed obvious -NH stretching and -NH bending absorption bands of amide group at approximately 3200 cm^{-1} and 1500 cm^{-1}, respectively. The C-H stretching of aromatic ring was shown at approximately 1600 cm^{-1} and the C-H bending of the aromatic ring could be observed at approximately 830 cm^{-1}. The absorption peaks of the C-O stretching could be observed at approximately 1070 cm^{-1}.

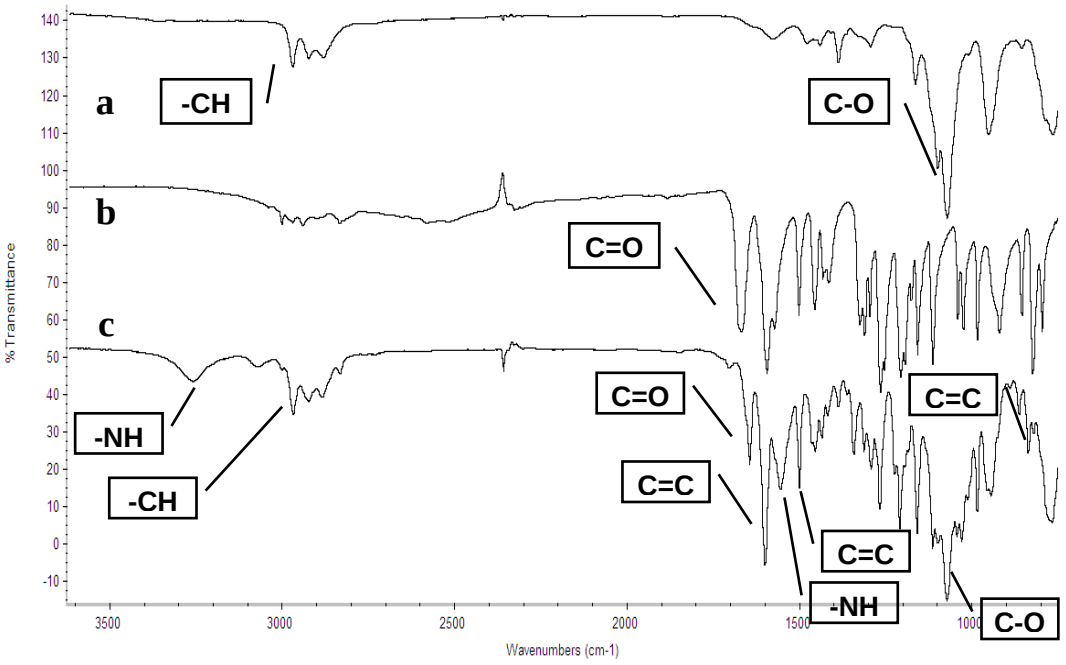

Figure 3.5 FT-IR spectra of 3-aminopropyltriethoxysilane **(APTES)** (a), 2,4-dimethoxycinnamic acid (b) and triethoxysilylpropyl-2,4-dimethoxycinnamamide, **(TES24C-1)** (c).

UV spectrum of **TES24C** showed obvious absorption the UVA region (λ_{max} ~ 291 and 322 nm). Thus, it could be concluded that 2,4-dimethoxycinnamic acid was successfully integrated into the monomeric structure.

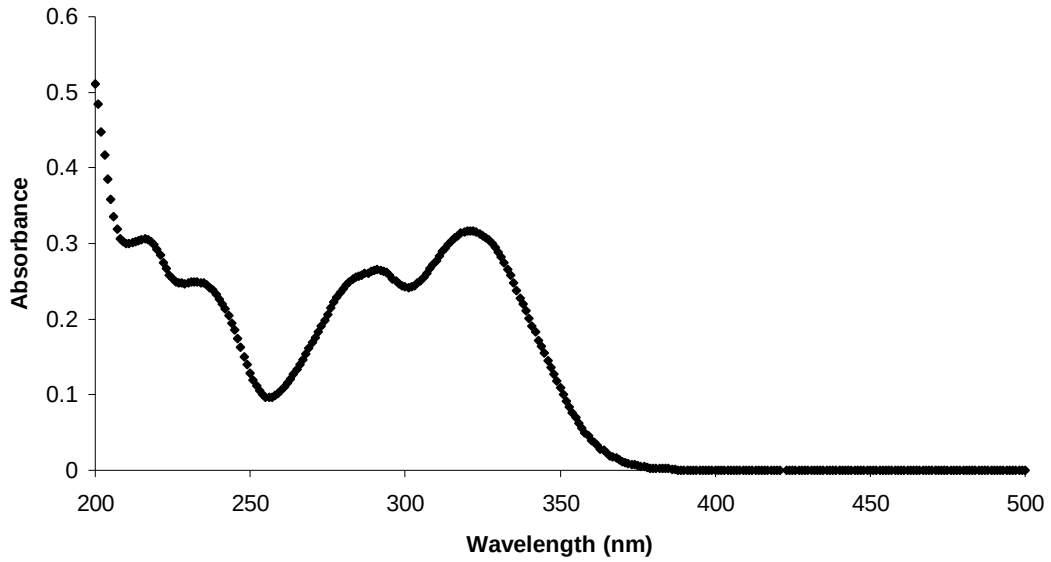

Figure 3.6 UV absorption spectrum of **TES24C-2** at molar absorptivity 1.24 x 10^{-5} M.

3.2 Polymerization and micro/nanospheres formation

In previous experiment (Section 3.1), UV-B and UV-A monomers were successfully synthesized. Here, both monomers were simultaneously polymerized and induced into particles using the two phase-organic-water dispersion system. The obtained particulate suspensions of poly[propyl-4-methoxycinnamamidesilsesquioxane] **(PTES4C)** and poly[propyl-2,4-dimethoxycinnamamidesilsesquioxane] **(PTES24C)** were subjected to dynamic light scattering and SEM analyses (see Appendix **A5-A12**).

Polymerization with catalysts (external catalysts): 0.1% HCl, 3% NH_4OH and 5% NH_4OH [4, 17]) and the process without catalyst (internal catalyst or self-catalysis process [19]) were compared.

3.2.1 Poly[propyl-4-methoxycinnamamidesilsesquioxane] (PTES4C) spheres

Processes with different catalysts were compared according to reaction time, synthesis yield, particle morphology and particles' polydispersity (Table 3.1). The acid-catalyst process gave highest synthesis yields and spheres with high polydispersity, but required longest reaction time. Self-catalysis process gave the second highest synthesis yield. This process required acceptable reaction time and gave more uniform spheres compared with other catalysts. The two basic conditions (3% NH_4OH and 5% NH_4OH) required reaction time of 1 h, however, gave lower yield than process other catalysts (Table 3.1).

Since amount of ethanol (solvent) used also affected product formation, the volume of ethanol used during the polymerization processes were evaluated at 10%, 20%, 30% and 40% (v/v). It was found that, the particle size increased with increasing volume of ethanol during particle formation but the high volume of ethanol inversely correlated with product yield (see Table 3.1 and Appendix **A5-A8**).

Thus, it can be concluded that the best condition to prepared **PTES4C** sphere was to use self-catalysis process at 20% (v/v) of ethanol. This process required acceptable reaction time, gave high synthesis yield and quite uniform spheres (diameter < 1 μm, PDI = 0.09).

Table 3.1 Particle characteristics of the synthesized poly[propyl-4-methoxy cinnamamidesilsesquioxane] **(PTES4C)** obtained from various catalysis processes, e.g. 0.1% HCl, self-catalysis, 3% NH_4OH and 5% NH_4OH with the ethanol effect (20%, 30% and 40% (v/v))

Catalysts	Reaction time	%EtOH (v/v)	Synthesis yields (%)	Average diameter [a] by SEM	Hydrodynamic diameters [b]	PDI [c]
0.1%HCl	14 days	20	87.38	449 ±190	610 ±10	0.23
		30	74.45	625 ± 282	798 ±10	0.23
		40	69.27	837 ±421	907 ±13	0.22
Self-catalysis	1 day	10	67.75	405 ±158	1049 ±89	0.44
		20	71.11	419 ±134	559 ±9	0.09
		30	64.21	788 ±269	1354 ±44	0.16
		40	x	x	x	x
3% NH_4OH	1 h	20	47.89	868 ±182	910 ±44	0.19
		30	41.99	1252 ±564	1987 ±203	0.16
		40	30.56	2361 ±402	3028 ±299	0.95
5% NH_4OH	1 h	20	37.30	513 ±137	687 ±54	0.34
		30	17.20	826 ±384	1456 ±81	0.25
		40	11.88	2254 ±212	2694 ±114	0.14

[a] Averaged from 100 spheres shown in a SEM photographs (Average size (nm) ± SD)

[b] Determined by dynamic light scatting (Average size (nm) ± SD)

X = uncompleted reaction

[c] The cumulants analysis -Polydispersity Index (PDI)

0 - 0.05: Only normally encountered with latex standards or particles made to be monodisperse
0.05 - 0.08: Nearly monodisperse sample. DLS cannot normally extract a distribution within this range
0.08 - 0.7: This is a mid-range polydispersity, it is the range over which the distribution algorithm based on NNLS best operates over

Greater than 0.7: Very polydisperse. Care should be taken in interpreting results as the sample may not be suitable for the technique, e.g. a sedimenting high size tail may be present

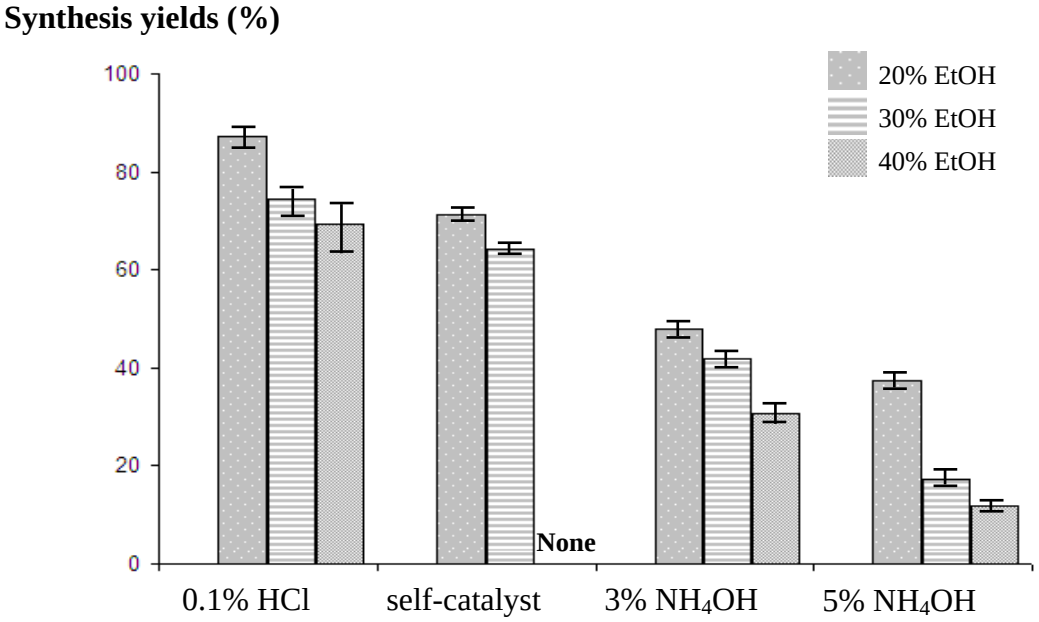

Figure 3.7 The synthesis yields (%) of poly[propyl-4-methoxycinnamamide silsesquioxane] **(PTES4C)** in various catalysis processes, e.g. 0.1% HCl, self-catalysis, 3% NH_4OH and 5% NH_4OH with the ethanol effect (20%, 30% and 40% (v/v)).

PTES4C products obtained from the self-catalysis process were characterized by UV-vis spectroscopy. **PTES4C** aqueous suspension and dry **PTES4C** showed obvious absorption in the UVB region (λ_{max} ~ 290 nm), (Figure 3.8). Thus, it can be concluded that **PTES4C** was the UVB absorptive agent.

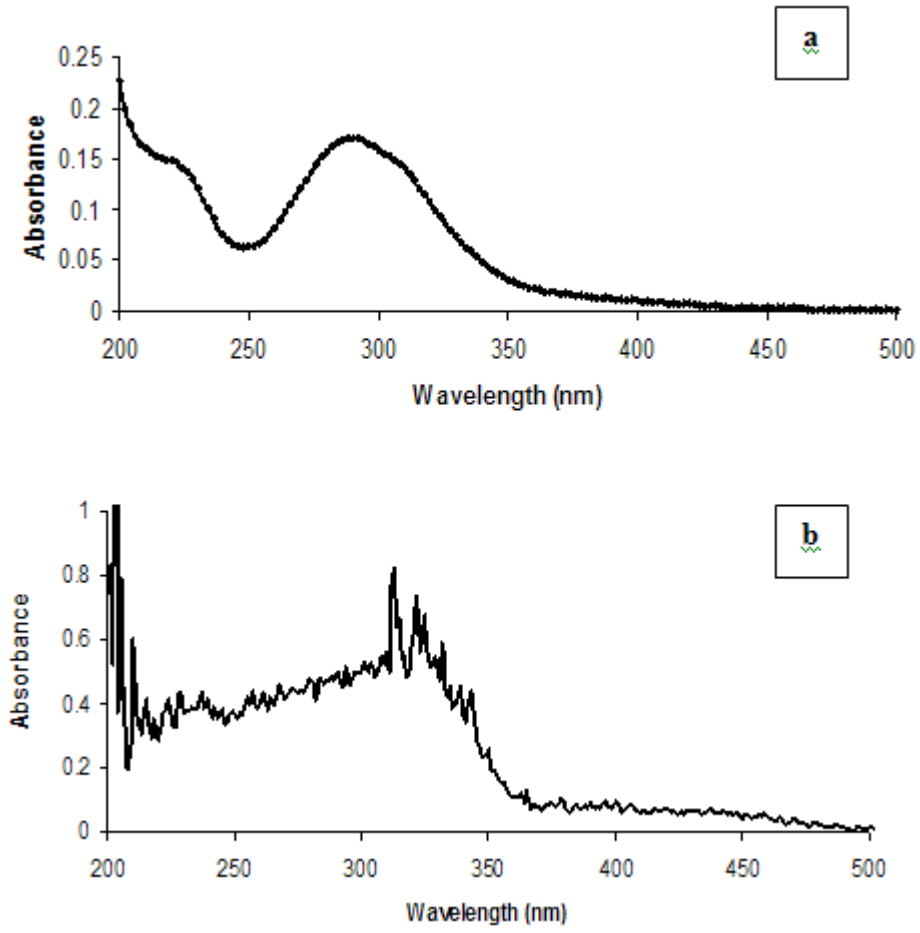

Figure 3.8 UV absorption spectrum of 80 ppm (in 20% ethanol) of **PTES4C** suspension product, **(a)** and 10 mg of **PTES4C** solid product, **(b)**

3.2.2 Poly[propyl-2,4-dimethoxycinnamamidesilsesquioxane] (PTES24C) spheres

Processes with different catalysts were compared according to reaction time, synthesis yield, particle morphology and particles' polydispersity (Table 3.2). The acid-catalyst-process gave highest synthesis yields and more uniform spheres (PDI = 0.13) but required longest reaction time. Self-catalysis process gave the second highest synthesis yield and required acceptable reaction time but gave spheres of broad range of diameter. Polymerization in basic condition (3% NH_4OH and 5% NH_4OH) required reaction time for 1 h but gave lower yield than other catalysts (Table 3.2).

Since amount of ethanol (solvent) used also affected product formation, the volume of ethanol used during the polymerization processes were evaluated at 10%, 20% and 30% (v/v). The result agreed well with previous experiment (section 3.2.1), the particle size increased with increasing volume of ethanol during particle formation but the high volume of ethanol inversely correlated with product yield (see Table 3.1 and Appendix **A9**-**A12**).

Although, the acid-catalyst-process gave highest synthesis yields and more uniform spheres but the self-catalysis process was the most convenient since neither washing nor neutralization were needed, required acceptable reaction time and gave high yield. Thus, it can be concluded that the best condition to prepared **PTES24C** sphere was the self-catalysis process at 10% (v/v) of ethanol.

Table 3.2 Particle characteristics of the synthesized poly[propyl-2,4-dimethoxy cinnamamidesilsesquioxane] **(PTES24C)** obtained from various catalysis processes, e.g. 0.1% HCl, self-catalysis, 3% NH_4OH and 5% NH_4OH with the ethanol effect (10%, 20% and 30% (v/v))

Catalysis	Reaction time	%EtOH (v/v)	Synthesis yields (%)	Average diameter [a] by SEM	Hydrodynamic diameters [b]	PDI [c]
0.1% HCl	3 days	10	77.91	576 ±228	768 ±12	0.13
		20	75.11	615 ±218	811 ±5	0.09
		30	56.70	755 ±134	1177 ±39	0.20
Self-catalysis	2 days	10	66.36	448 ±166	N/A	N/A
		20	64.48	465 ±191	N/A	N/A
		30	x	x	x	x
3% NH_4OH	1 h	10	24.95	451 ±148	482 ±17	0.22
		20	38.50	956 ±391	929 ±22	0.10
		30	31.64	1792 ±677	2142 ±122	0.28
5% NH_4OH	1 h	10	22.34	402 ±192	471 ±16	0.24
		20	40.68	535 ±204	706 ±9	0.14
		30	20.05	1557 ±332	1316 ±26	0.11

[a] Averaged from 100 spheres shown in a SEM photographs (Average size (nm) $\pm$ SD)

[b] Determined by dynamic light scatting (Average size (nm) $\pm$ SD)

X = uncompleted reaction

[c] The cumulants analysis -Polydispersity Index (PDI)

0 - 0.05: Only normally encountered with latex standards or particles made to be monodisperse
0.05 - 0.08: Nearly monodisperse sample. DLS cannot normally extract a distribution within this range
0.08 - 0.7: This is a mid-range polydispersity, it is the range over which the distribution algorithm based on NNLS best operates over
Greater than 0.7: Very polydisperse. Care should be taken in interpreting results as the sample may not be suitable for the technique, e.g. a sedimenting high size tail may be present

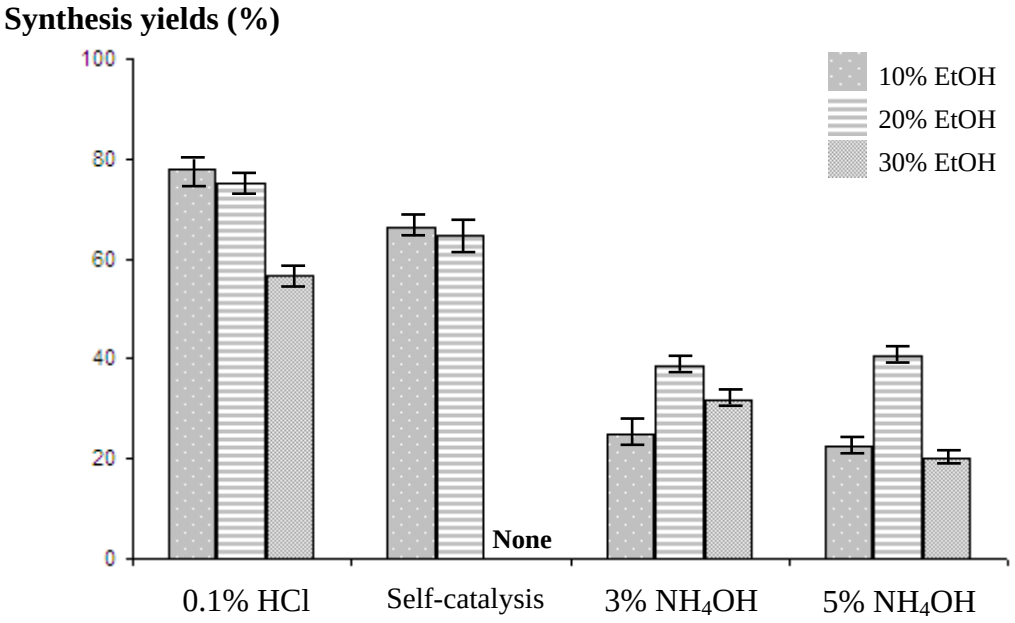

Figure 3.9 The synthesis yields (%) of poly[propyl-2,4-dimethoxycinnamamide silsesquioxane] **(PTES24C)** of various catalysis processes, e.g. 0.1% HCl, self-catalysis, 3% NH_4OH and 5% NH_4OH with the ethanol effect (10%, 20% and 30% (v/v)).

PTES24C products obtained from the self-catalysis process were also characterized by UV-vis spectroscopy. Both aqueous suspension of **PTES24C** and dry **PTES24C** showed obvious absorption in the UVA region (λ_{max} ~ 292 and 322 nm), (Figure 3.10). Thus, it can be concluded that **PTES24C** was the UVA region absorptive agent.

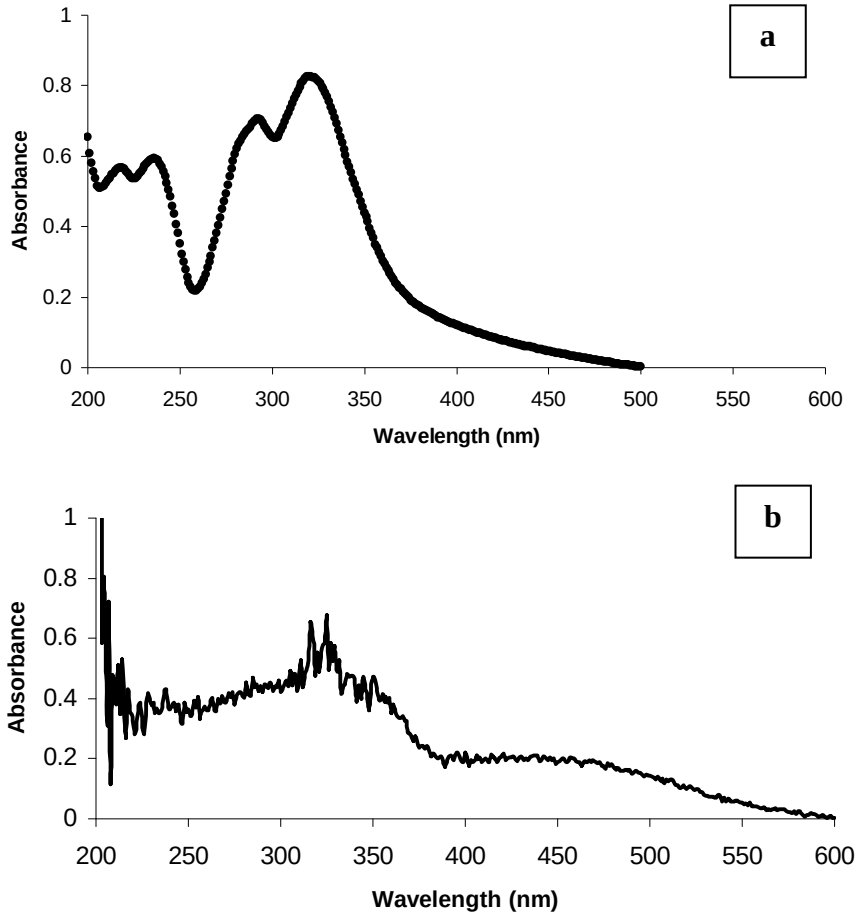

Figure 3.10 UV absorption spectrum of 200 ppm (in 20% ethanol) of **PTES24C** suspension product, **(a)** and 10 mg of **PTES24C** solid product, **(b)**.

Therefore it can be concluded that polymerization was successfully carried out using catalysts (external catalysts): 0.1% HCl, 3% NH_4OH and 5% NH_4OH and the process without added catalyst (internal catalyst or self-catalysis process), although with different effectiveness. Different mechanisms are responsible for different processes. The mechanisms are present in the following paragraphs.

3.2.3 Polymerization mechanism

Polymerization mechanism of the three catalysts discussed above, have been previously proposed by Leyden and coworkers. The acid-catalyst hydrolysis of ethoxysilanes proceeds through a S_N2 mechanism (Figure 3.11). First, H^+ protonates the oxygen atom of the ethoxygroup and a water molecule performs a nucleophilic attack at silicon atom to give an oxonium ion intermediate. The obtained ROH was a good leaving group [8, 27].

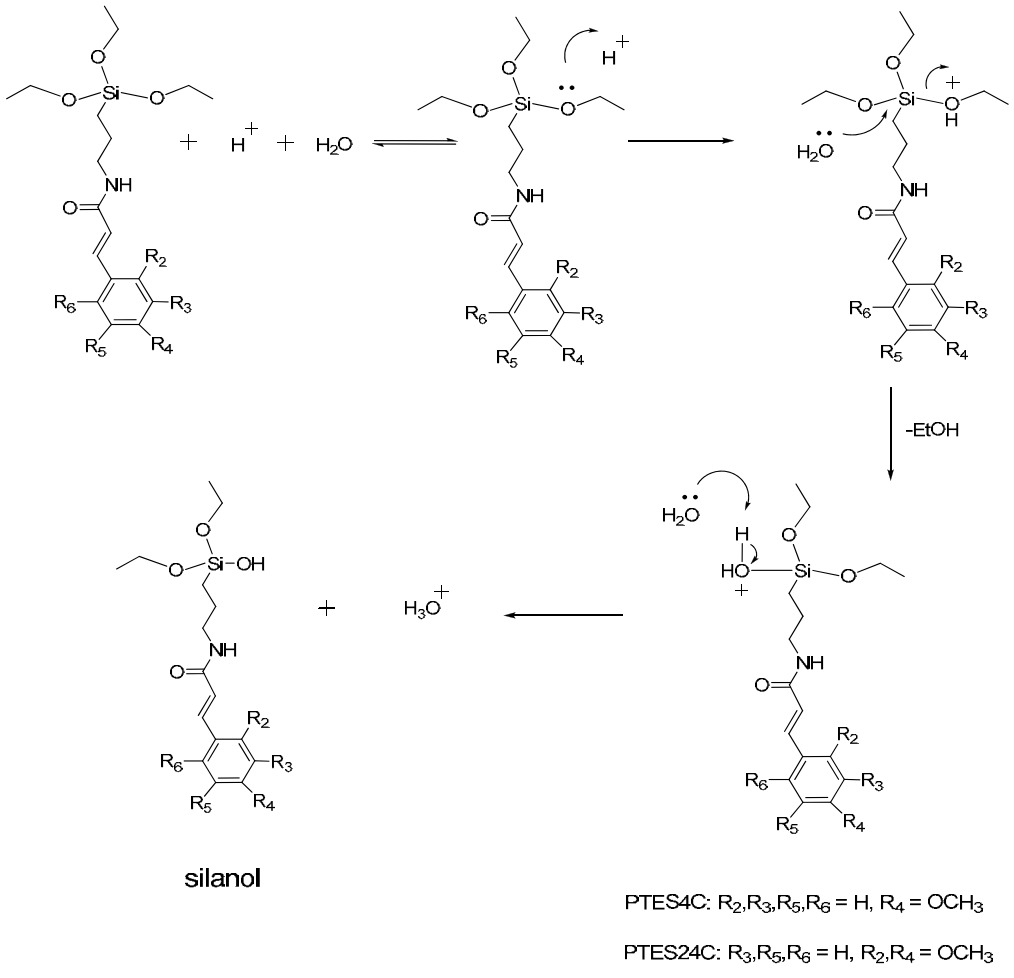

Figure 3.11 Proposed mechanism for the acid catalyst hydrolysis.

The base catalyst hydrolysis perhaps to proceed via a bimolecular nucleophilic substitution reaction (S_N2) (Figure 3.12). In the first step of this reaction, the base (OH^-) attacks a silicon atom on an ethoxysilane. The protonation changes the leaving group from RO^- to ROH which is a good leaving group [8, 27].

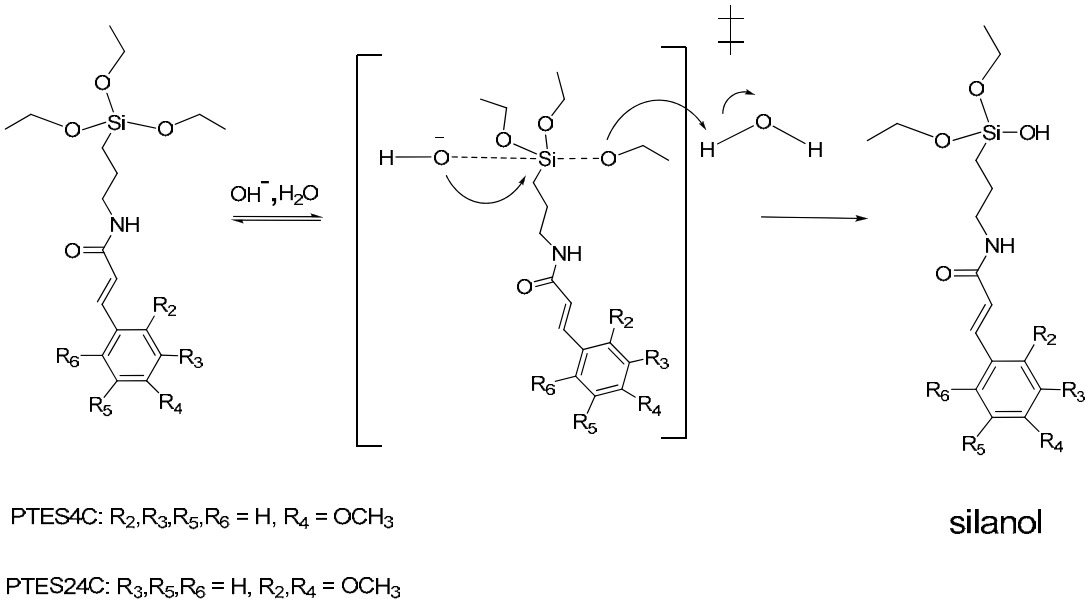

Figure 3.12 Proposed mechanism for the base catalyst hydrolysis.

The self-catalysis hydrolysis proceeds are involved basic property of APTES and water are nucleophilic attack at the central silicon atom. The protonation changes the leaving group from RO^- to ROH which is a good leaving group (Figure 3.13).

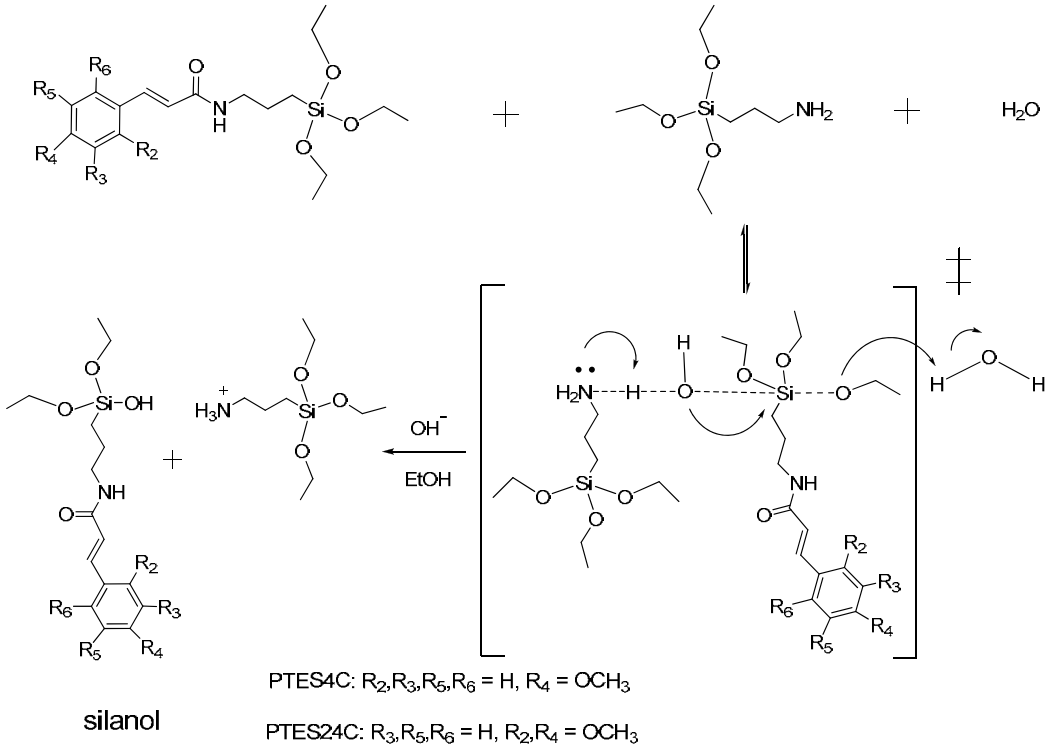

Figure 3.13 Proposed mechanism for the self-catalysis hydrolysis.

The condensation may be acid or base catalyzed. The silanol molecules condense to form silanol bonds involved water-condensation, with release of water and alcohol-condensation, with releasing an alcohol [27, 28].

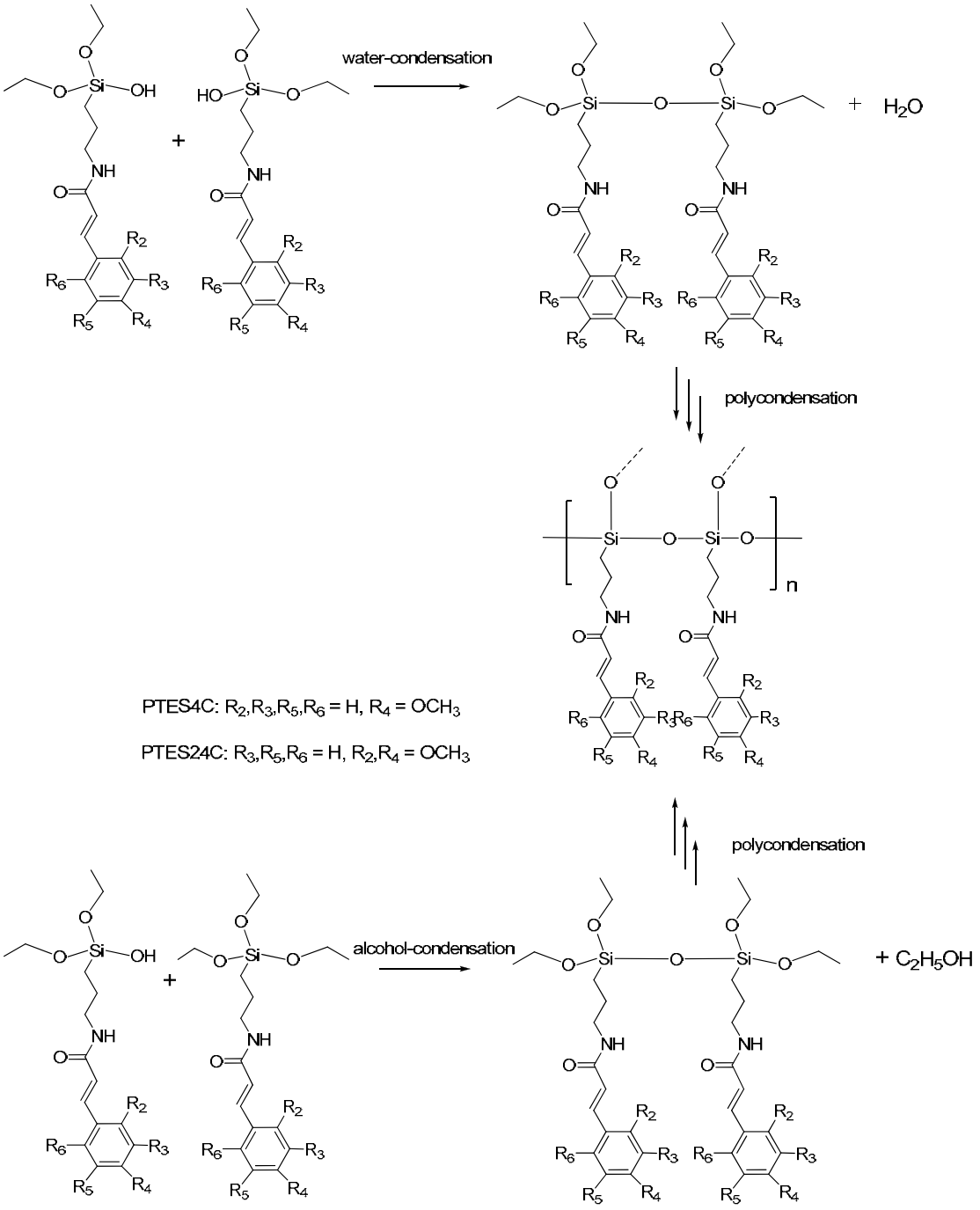

Figure 3.14 Polycondensation reactions of silanol molecules through water-condensation and alcohol-condensation.

In addition, the study demonstrated that the amount of ethanol used during polymerization affected the synthesis yield and particle size. The particle size increased with increasing volume of ethanol during particle formation but the volume of ethanol inversely correlated with the product yield (see Table 3.1-3.2); the volume of ethanol increased, esterification of monomer increased. This could be explained through the retardation of dimerigation (Fig 3.15). Less dimerigation then delayed further condensation [29].

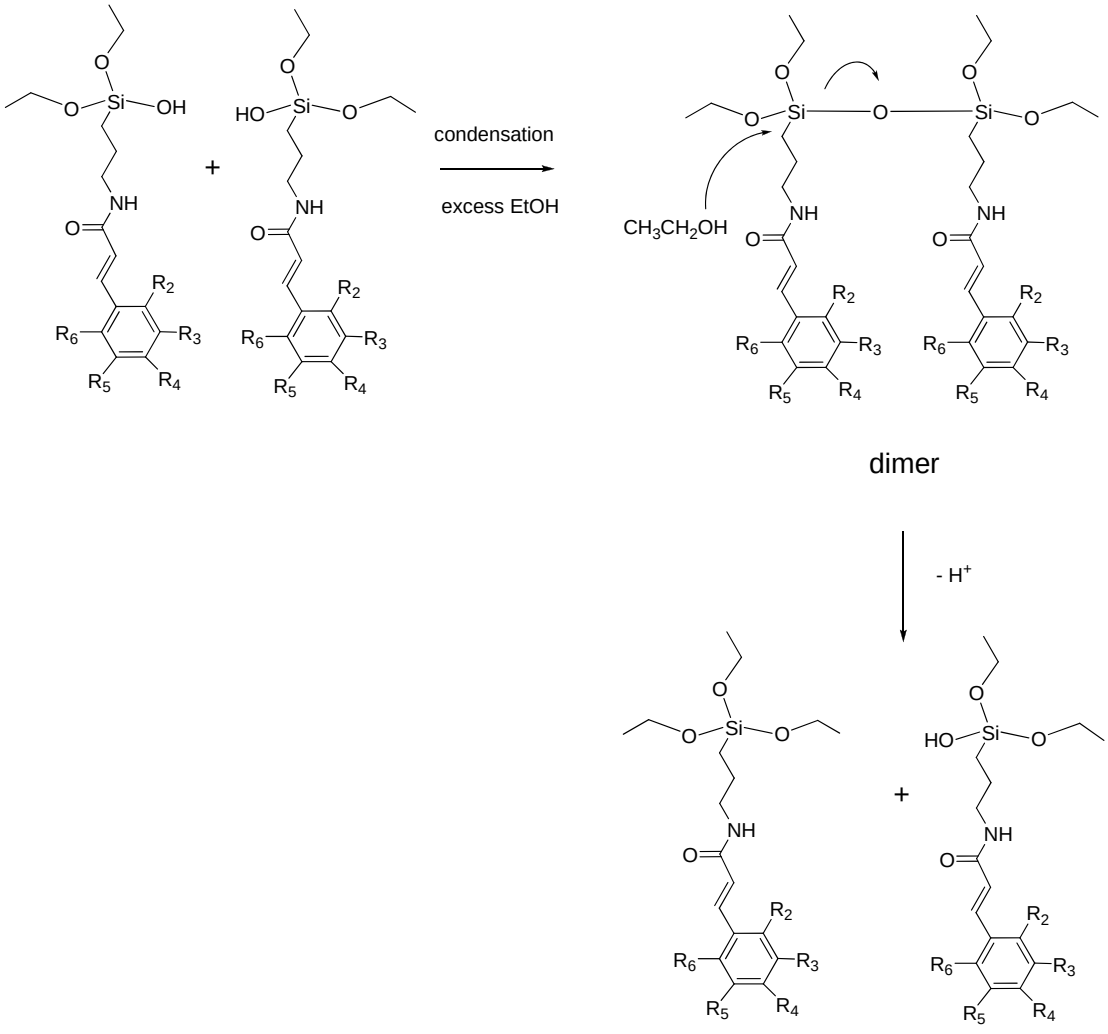

Figure 3.15 Proposed mechanism for ethanol affects to polymerization processes.

3.3 Effects of monomer concentration during the particle formation

In previous experiment (Section 3.2.1 and 3.2.2), the best condition to prepared **PTES4C** and **PTES24C** spheres were 20% and 10% ethanol, respectively. These conditions were used in the following experiments in which concentration of monomer was optimized.

In previous experiment, all the suspension products were prepared at the final monomer concentration of 0.02 mg/ml. Therefore this experiment, the preparation of **PTES4C** and **PTES24C** were studied at higher concentrations of the hybrid monomers: 0.04 and 0.06 g/ml (see chapter II, Table 2.2-2.3 for condition). Only the best polymerization which is self-catalysis was investigated. The obtained particulate suspensions were subjected to dynamic light scattering and SEM analyses.

3.3.1 Poly[propyl-4-methoxycinnamamidesilsesquioxane] (PTES4C) spheres

The particles of **PTES4C** could be obtained from the process carried out at 0.02, 0.04 and 0.06 g/ml of **TES4C** hybrid monomer (Figure 3.16). However, higher monomer concentration gave lower yield due to the formation of sticky masses (by product) (Table 3.3).

Table 3.3 Characteristics of **PTES4C** particles prepared at different monomer concentration.

Concentration of TES4C hybrids monomer (g/ml)	Synthesis yields (%)	Average diameter [a] by SEM	Hydrodynamic diameters [b]	PDI
0.02	71.90	419 ±134	559 ±9	0.10
0.04	53.76	437 ±177	564 ±8	0.15
0.06	41.34	465 ±159	566 ±6	0.14

[a] Averaged from 100 spheres shown in a SEM photographs (Average size ± SD)

[b] Determined by dynamic light scatting (Average size ± SD)

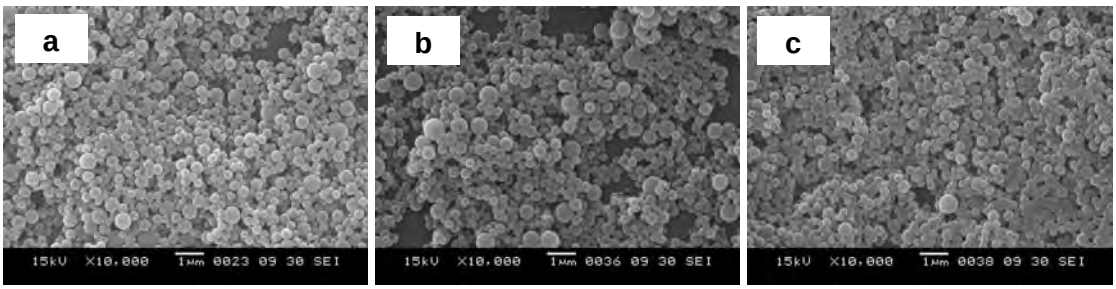

Figure 3.16 Scanning electron micrographs of **PTES4C** spheres prepared at the monomer concentrations of 0.02 (a), 0.04 g/ml (b) and 0.06 g/ml (c).

It can be seen (Table 3.3) that the yield decreased with increased monomer concentration. Thus, the best condition to prepared **PTES4C** sphere was 0.02 g/ml of **TES4C** hybrid monomer concentration with 20% ethanol under self-catalysis process.

3.3.2 Poly[propyl-2,4-dimethoxycinnamamidesilsesquioxane] (PTES24C) spheres

The particles of **PTES24C** could be obtained from the process carried out at 0.02 and 0.04 g/ml but not at 0.06 g/ml of **TES4C** hybrid monomer (Figure 3.17). However, higher monomer concentration gave lower yield due to the formation of sticky masses (Table 3.4).

The particle size of **PTES24C** spheres could not be analyzed with dynamic light scattering (the particles agglomerated severely) but the particle size could be visualized by SEM (Table 3.4).

Table 3.4 Characteristics of **PTES24C** particles prepared at different monomer concentration.

Concentration of TES24C hybrids monomer (g/ml)	Synthesis yields (%)	Average diameter [a] by SEM	Hydrodynamic diameters [b]	PDI
0.02	67.95	448 ±166	N/A	N/A
0.04	51.70	409 ±129	N/A	N/A
0.06	x	x	x	x

[*] Averaged from 100 spheres shown in a SEM photographs.

X = uncompleted reaction

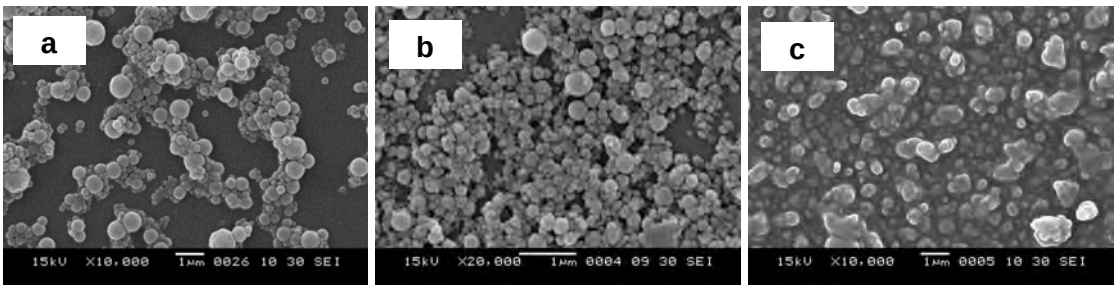

Figure 3.17 Scanning electron micrographs of **PTES24C** spheres prepared at the concentrations of 0.02 g/ml (a), 0.04 g/ml (b) and 0.06 g/ml (c).

Thus, the best condition to prepared **PTES24C** sphere was 0.02 g/ml of **TES24C** hybrid monomer with 10% ethanol under self-catalysis process.

3.4 Effects of surfactant

Sine particle formation was carried out simultaneously during the polymerization in a two-phase-organic-water condition, it was reasonable to see if surfactant could help the dispersion of the formed spheres in water (hence uniformity of the particles).

In previous experiment (Section 3.3.1 and 3.3.2), best condition to prepared **PTES4C** and **PTES24C** spheres were at 0.02 g/ml of monomer with 20% and 10% ethanol, respectively under the self-catalysis process. The condition was as therefore, used in the following experiment. Triton X-100 was chosen as a surfactant because it is a nonionic, non-toxic surfactant used commonly in many biological preparations [30].

Then, the aqueous suspension of the obtained particles was subjected to SEM and dynamic light scattering analyses.

The preparation of **PTES4C** spheres in a presence of surfactant gave a lot of sticky masses (Figure 3.18).

The preparation of **PTES24C** spheres in a presence of surfactant gave uniform spheres with the synthesis yield of 73.15% and average particle size of 228 ±30 nm (Figure 3.19).

Thus it was conclude that **PTES24C** spheres should be prepared under the presence of Triton X-100 while **PTES24C** spheres preparation should require no surfactant.

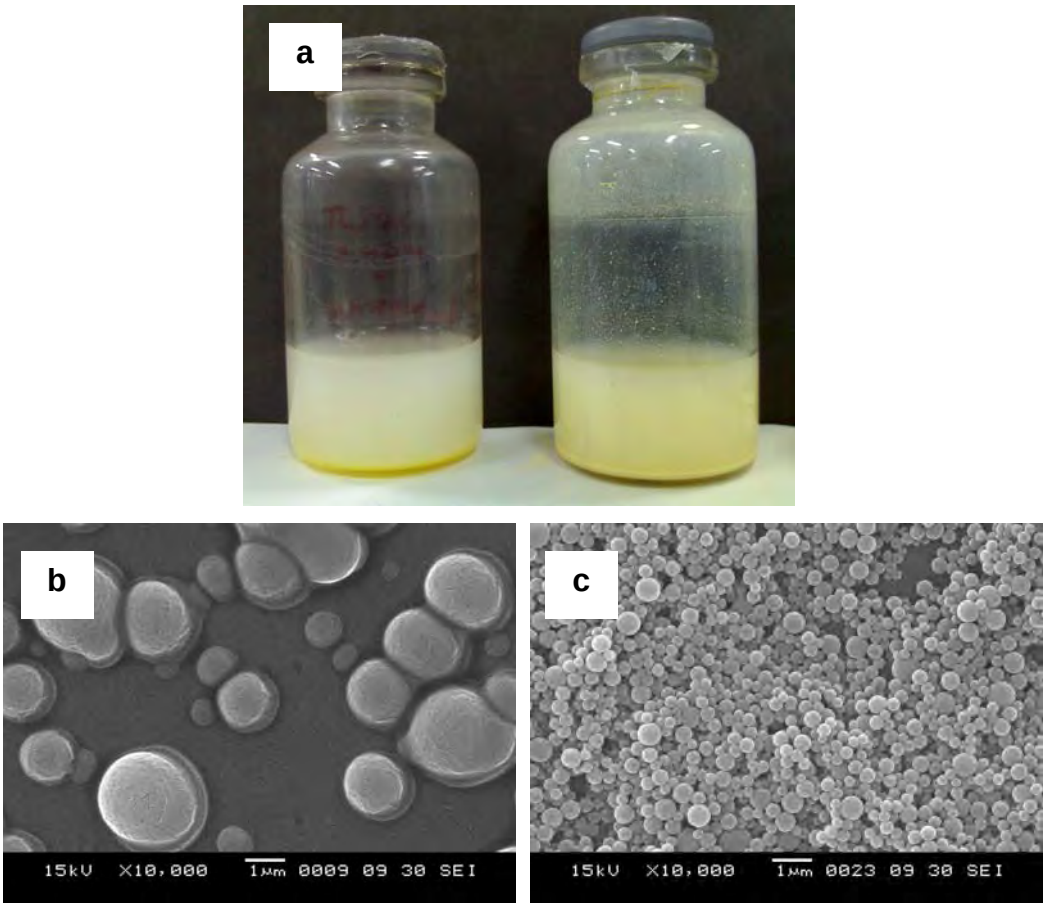

Figure 3.18 Pictures of **PTES4C** products obtained with (a, left) and with out (a, right) the presence of Triton X-100 in the preparation process. SEM photographs of **PTES4C** obtained with (b) and with out (c) Triton X-100.

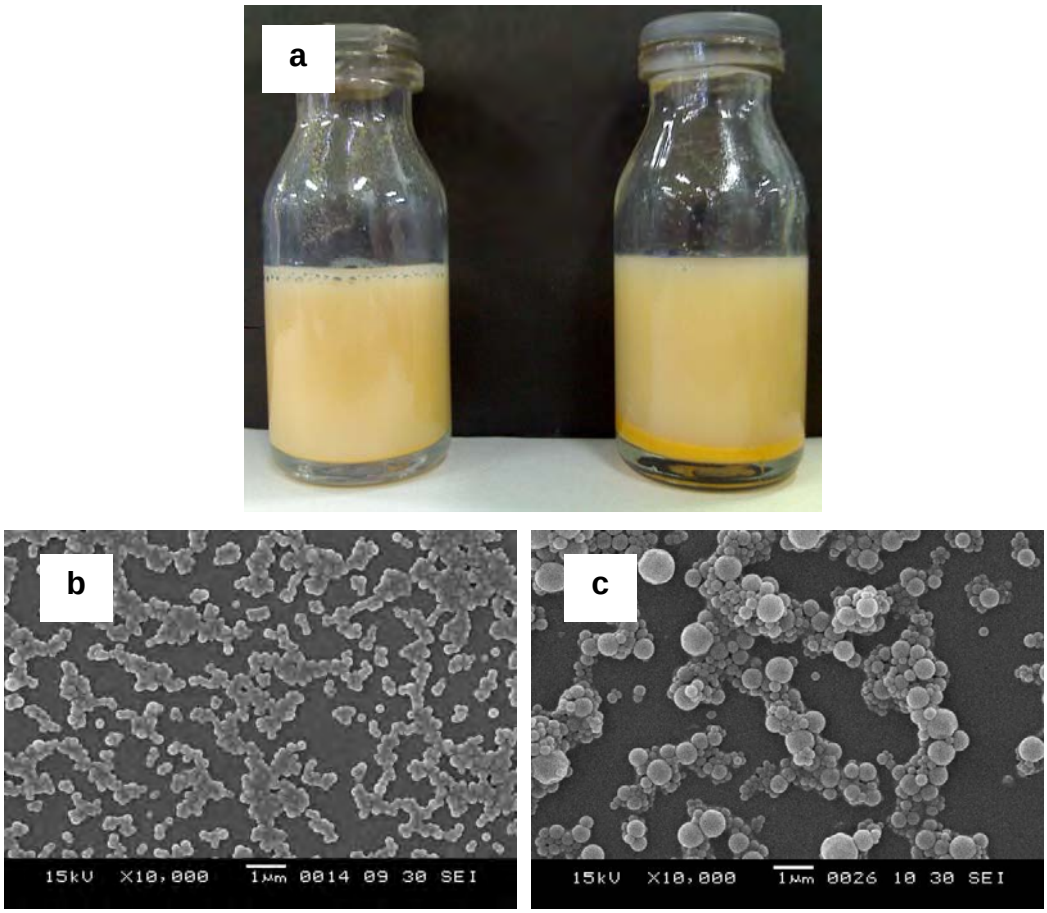

Figure 3.19 Pictures of **PTES24C** products obtained with (a, left) and with out (a, right) the presence of Triton X-100 in the preparation process. SEM photographs of **PTES24C** obtained with (b) and with out (c) Triton X-100.

3.5 Encapsulation processes

As described earlier, the best condition to prepared **PTES4C** and **PTES24C** spheres was at 0.02 g/ml monomer with 20% and 10% ethanol, respectively under self-catalysis process. These conditions were used in the following experiments in which encapsulation were demonstrated.

The 2-ethylhexyl-4-methoxycinnamate (**EHMC**) (at concentration of 0.01 g/ml) was chosen as a model compound for encapsulation. The encapsulation efficiency and loading capacity of **EHMC** was evaluated by extracting the encapsulated **EHMC** from the spheres using hexane and quantitating the extract with UV-absorptive spectrophotometry (see chapter II, Section 2.7).

The obtained micro/nanoparticulate suspension was subjected to SEM and TEM analyses. Agglomeration amongst the spheres prevented the DLS analysis of the product.

3.5.1 Encapsulation of 2-ethylhexyl-4-methoxycinnamate into poly[propyl-4-methoxycinnamamidesilsesquioxane] (PTES4C) spheres.

PTES4C spheres were evaluated for their possible role as carrier. The **EHMC**-encapsulated **PTES4C** particles gave the best encapsulation efficiency of 61.54% at **EHMC** loading of 20.86% (weight of **EHMC**/weight of **EHMC**-encapsulated **PTES4C** particles). Scanning electron micrographs indicated that the particles were spherical with an average particle size of 560 ±40 nm (Figure 3.20).

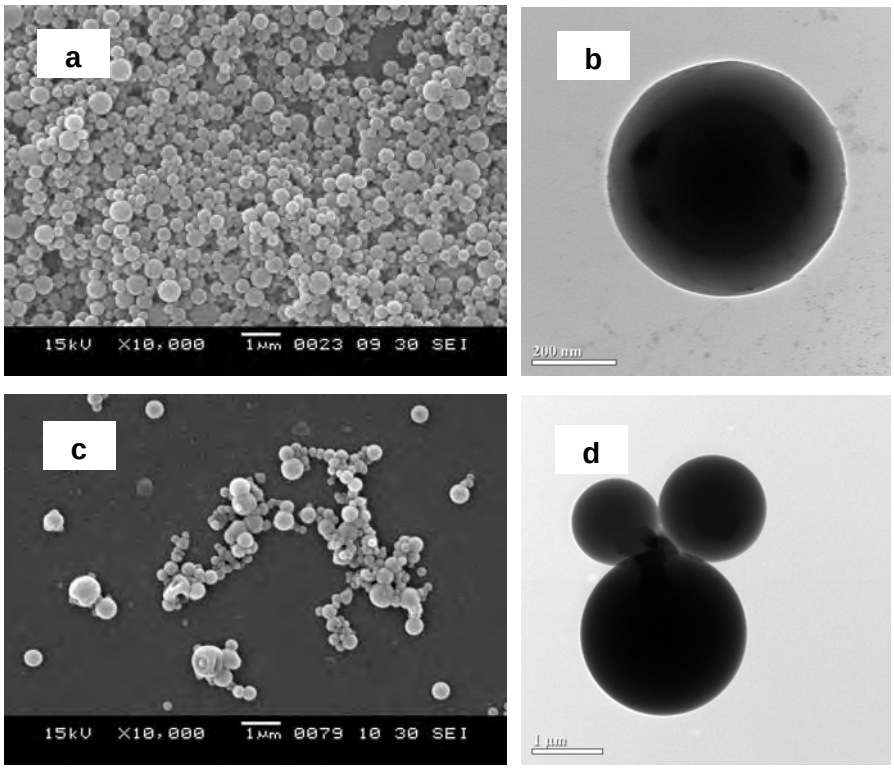

Figure 3.20 Morphology of non-encapsulated **PTES4C** particles (a, b) and **EHMC**-encapsulated **PTES4C** particles (c, d). The images were obtained by SEM (a, c) and TEM (b, d).

3.5.2 Encapsulation of 2-ethylhexyl-4-methoxycinnamate into poly[propyl-2,4-dimethoxycinnamamidesilsesquioxane] (PTES24C) spheres.

The study demonstrates, **EHMC**-encapsulated in **PTES24C** cannot form particles and gave detectable precipitates (Figure 3.21, (b)). However**, PTES24C** spheres were evaluated for their possible role as carrier in a presence of surfactant (5% v/v of Triton X-100).

PTES24C spheres were evaluated for their possible role as carrier. The **EHMC**-encapsulated **PTES24C** particles gave the best encapsulation efficiency of 31.87% at **EHMC** loading of 10.17% (weight of **EHMC**/weight of **EHMC**-encapsulated **PTES24C** particles). Scanning electron micrographs indicated that the particles were spherical with an average particle size of 219 ±30 nm (Figure 3.21, (c)).

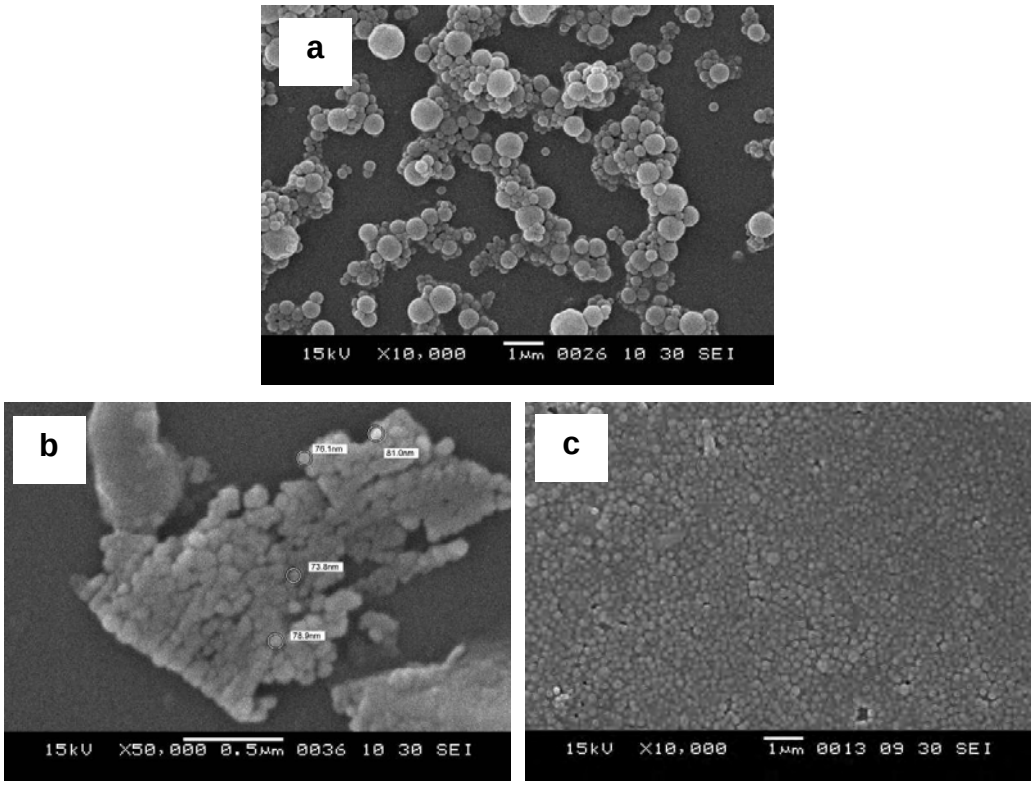

Figure 3.21 SEM images of non-encapsulated **PTES24C** particles (a), **EHMC**-encapsulated **PTES24C** particles (b) and **EHMC**-encapsulated **PTES24C** particles in a presence of surfactant (c).

3.6 Measurement of a solar protection factor (SPF)

The solar protection factor (SPF) and UV-A protection factor (UV-A PF) of poly[propyl-4-methoxycinnamamidesilsesquioxane] **(PTES4C)** and poly[propyl-2,4-dimethoxycinnamamide silsesquioxane] **(PTES24C)** spheres were carried out and compared with 2-ethyl-hexyl-4-trimethoxycinnamate **(EHMC)**, a widely used sunscreening active. All samples were prepared with 10% (w/w) of active ingredients in cream base [31] (Figure 3.22) and were subjected to the measurement (Table 3.5). The result indicated that **PTES4C** and **PTES24C** were good UV absorber.

Table 3.5 The solar protection factor (SPF) and UV-A protection factor (UV-A PF) values of poly[propyl-4-methoxycinnamamidesilsesquioxane] (**PTES4C)**, poly[propyl-2,4-dimethoxycinnamamidesilsesquioxane] **(PTES24C)** and 2-ethyl-hexyl-4-trimethoxy cinnamate (EHMC).

Compounds	SPF	SD	UV-A PF	SD
PTES4C	21.42-23.18	1.47-2.00	8.04	0.76
PTES24C	12.76-13.61	1.13-1.87	4.94	0.58
EHMC	19.51-20.12	1.03-1.63	7.27	1.16

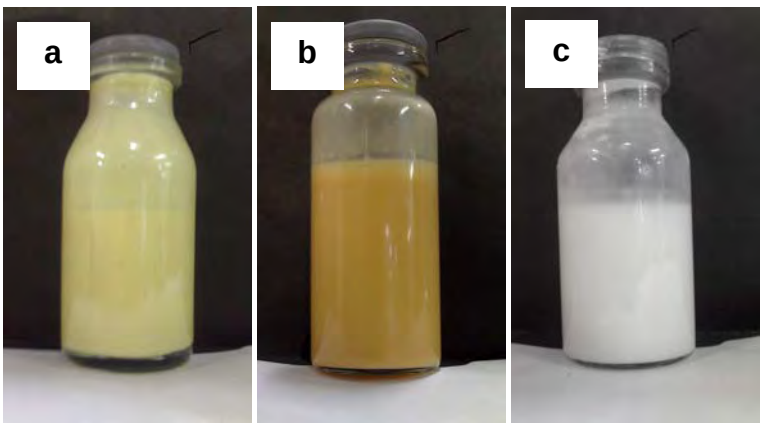

Figure 3.22 The creams containing poly[propyl-4-methoxycinnamamidesilsesqui-oxane] **(PTES4C)** (a), poly[propyl-2,4-dimethoxycinnamamide silsesqui oxane] **(PTES24C)** (b) and 2-ethyl-hexyl-4-trimethoxycinnamate **(EHMC)** (c).

3.7 Redispersion and particle stability from various catalysts

As described earlier, the best condition to prepared **PTES4C** and **PTES24C** spheres was at 0.02 g/ml monomer with 20% and 10% ethanol, respectively under self-catalysis process. These conditions were used in the following experiments in which Redispersion and particle stability were demonstrated.

The redispersion of **PTES4C** spheres obtained from 0.1% HCl and self-catalysis process, in water showed no detectable precipitate but the redispersion of spheres obtained from 3% NH_4OH and 5% NH_4OH, gave detectable precipitates after 1 h (Figure 3.23). SEM analyses revealed that all precipitates were agglomerated particles (Appendix **A5-A8**).

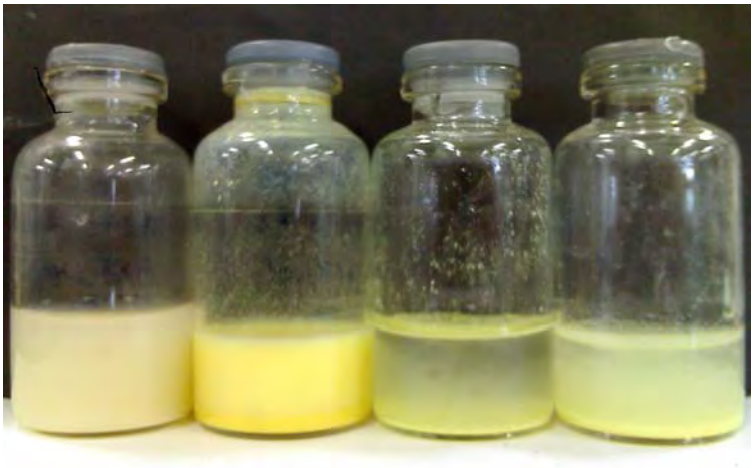

0.1% HCl **self-catalysis** **3% NH_4OH** **5% NH_4OH**

Figure 3.23 Pictures of the redispersed **PTES4C** particles prepared at0.01 g/ml.

The redispersion of **PTES24C** spheres obtained from 0.1% HCl process, in water showed no detectable precipitate but the redispersion of spheres obtained from self-catalysis process, 3% NH_4OH and 5% NH_4OH, gave detectable precipitates after 1 h (Figure 3.24). SEM analyses revealed that all precipitates were agglomerated particles (Appendix **A9-A12**).

0.1% HCl Self-catalysis 3%NH_4OH 5%NH_4OH

Figure 3.24 Pictures of the redispersed **PTES24C** particles prepared at0.01 g/ml.

Therefore, best condition to synthesized **PTES4C** spheres was 0.02 g/ml monomer at 20% ethanol while that of **PTES24C** spheres was 0.02 g/ml monomer at 10% ethanol.

CHAPTER IV

CONCLUSION

Polysilsesquioxane micro/nanospheres with UV absorption property could be prepared successfully using the hybrid monomers, triethoxysilylpropyl-4-methoxy cinnamamide and triethoxysilylpropyl-2,4-dimethoxycinnamamide. Polymerization and particles formation was carried in the two phase-organic-water dispersed condition.

It was found that the catalysis types and volume of solvent used during the particle formation, affected particle size and product yield. The best condition to produce the UV-B absorptive spheres (**PTES4C** was 0.02 g/ml of **TES4C** hybrid monomer concentration with 20% ethanol under self-catalysis process.) while the best condition to produce the UV-A absorptive spheres (**PTES24C** was 0.02 g/ml of **TES24C** hybrid monomer with 10% ethanol under self-catalysis process). Both spheres showed UV-B and UV-A screening property when incorporated in cream base formulation.

Encapsulation of 2-ethylhexyl-4-methoxycinnamate into poly[propyl-4-methoxycinnamamidesilsesquioxane], **PTES4C** and poly[propyl-2,4-dimethoxy cinnamamidesilsesquioxane], **PTES24C** particles could be carried out successfully at 61.54% encapsulation efficiency (20.86% loading) and 31.87% encapsulation efficiency (10.17% loading), respectively.

REFERENCES

[1] Sanchez, C.; Beatriz, J.; Belleville, P.; and Popall, M., Applications of hybrid organic-inorganic nanocomposites. *Journal of Materials Chemistry* 15(2005): 3559-3592.

[2] Baney, R. H.; Itoh, M.; Sakakibara, A.; and Suzuki, T., Silsesquioxanes. *Chemical Reviews* 95, 5(1995): 1409-1430.

[3] Barbé, C.; Kong, L.; Finnie, K.; Calleja, S.; Hanna, J.; Drabarek, E.; Cassidy, D.; and Blackford, M., Sol–gel matrices for controlled release: from macro to nano using emulsion polymerisation. *Journal of Sol-Gel Science and Technology* 46, 3(2008): 393-409.

[4] Loy, D. A.; and Shea, K. J., Bridged Polysilsesquioxanes. Highly Porous Hybrid Organic-Inorganic Materials. *Chemical Reviews* 95, 5(1995): 1431-1442.

[5] Shea, K. J.; and Loy, D. A., Bridged Polysilsesquioxanes. Molecular-Engineered Hybrid Organic-Inorganic Materials. *Chemistry of Materials* 13, 10(2001): 3306-3319.

[6] Inagaki, S.; Guan, S.; Fukushima, Y.; Ohsuna, T.; and Terasaki, O., Novel Mesoporous Materials with a Uniform Distribution of Organic Groups and Inorganic Oxide in Their Frameworks. *Journal of the American Chemical Society* 121, 41(1999): 9611-9614.

[7] Scott, D. W., Thermal Rearrangement of Branched-Chain Methylpolysiloxanes1. *Journal of the American Chemical Society* 68, 3(1946): 356-358.

[8] Vansant, E. F.; Van Der Voort, P.; and Vrancken, K. C., *Characterization and Chemical Modification of the Silica Surface*. 2nd ed. Netherlands: Elsevier, 1995.

[9] Feher, F. J.; Budzichowski, T. A.; Blanski, R. L.; Weller, K. J.; and Ziller, J. W., Facile syntheses of new incompletely condensed polyhedral oligosilsesquioxanes: $[(c\text{-}C_5H_9)_7Si_7O_9(OH)_3]$, $[(c\text{-}C_7H_{13})_7Si_7O_9(OH)_3]$, and $[(c\text{-}C_7H_{13})_6Si_6O_7(OH)_4]$. *Organometallics* 10, 7(1991): 2526-2528.

[10] Abbenhuis, H. C. L. *Hybrid Catalysis*[Online]. 2006. Available from: www. hybridcatalysis.com [2009, March 31]

[11] Silicones Environmental, Health and Safety Council. *Aminosilanes Category Justification*[Online].2000. Available from: www.epa.gov/hpv/pubs/ summaries/dinapcat/c15766tp.pdf [2009, May 15]

[12] Hernandez, O., *3-Aminopropyltriethoxysilane CAS N°:919-30-2*[Online].2003. Available from: www.inchem.org/documents/sids/sids/ 919302.pdf [2009. May 28]

[13] Monhaphol, T.; Albinsson, B.; and Wanichwecharungruang, S. P., 2-Ethylhexyl-2,4,5-trimethoxycinnamate and di-(2-ethylhexyl)-2,4,5-trimethoxy benzalmalonate as novel UVA filters. Journal of Pharmacy and Pharmacology 59(2007): 279-288.

[14] Shi, Y.; Chen, Q. X.; Wang, Q.; Song, K. K.; and Qiu, L., Inhibitory effects of cinnamic acid and its derivatives on the diphenolase activity of mushroom (Agaricus bisporus) tyrosinase. *Food Chemistry* 92, 4(2005): 707-712.

[15] Adisakwattana, S.; Sookkongwaree, K.; Roengsumran, S.; Petsom, A.; Ngamrojnavanich, N.; Chavasiri, W.; Deesamer, S.; and Yibchok-anun, S., Structure-activity relationships of trans-cinnamic acid derivatives on [alpha]-glucosidase inhibition. *Bioorganic & Medicinal Chemistry Letters* 14, 11(2004): 2893-2896.

[16] Thitinum Monhaphol. *Synthesis of cinnamate derivatives and related compounds as novel UV filters.* Master's Thesis. Department of Chemistry, Graduate School, Chulalongkorn University, 2002.

[17] Stober, W.; Fink, A.; and Bohn, E., Controlled growth of monodisperse silica spheres in the micron size range. *Journal of Colloid and Interface Science* 26, 1(1968): 62-69.

[18] Choi, J. Y.; Kim, C. H.; and Kim, D. K., Formation and Characterization of Monodisperse, Spherical Organo-Silica Powders from Organo-Alkoxysilane-Water System. *Journal of the American Ceramic Society* 81, 5(1998): 1184-1188.

[19] Ottenbrite, R. M.; Wall, J. S.; and Siddiqui, J. A., Self-Catalyzed Synthesis of Organo-Silica Nanoparticles. *Journal of the American Ceramic Society* 83, 12(2000): 3214-3215.

[20] Lapidot, N.; Gans, O.; Biagini, F.; Sosonkin, L.; and Rottman, C., Advanced sunscreens: UV absorbers encapsulated in sol-gel glass microcapsules. 26(2003): 67-82.

[21] Kim, Y.B.; Yoon, K.S.; Kim, M.J.; Kim, M.J.; and Leem, M.S., Poly(silsesquioxane) spherical particle containing ultraviolet light-absorbing group and manufacturing method thereof. *International Application Published under the patent cooperation treaty, WO 2005/105028.* (10 November 2005):

[22] Zhou, J.; Wang, L.; Dong, X.; Chen, T.; Yang, Q.; Chen, C.; and Chen, X., Preparation of organic/inorganic hybrid nanoballs using aggregates of PTMSPMA-b-PSMA-Fc-PSMA-b-PTMSPMA block copolymers as precursors. *Nanotechnology* 17, 11(2006): 2745-2751.

[23] Khiterer, M.; and Shea, K. J., Spherical, Monodisperse, Functional Bridged Polysilsesquioxane Nanoparticles. *Nano Letters* 7, 9(2007): 2684-2687.

[24] Martin, H. J.; Schulz, K. H.; Bumgardner, J. D.; and Walters, K. B., XPS study on the use of 3-aminopropyltriethoxysilane to bond chitosan to a titanium surface. *American Chemical Society* 23(2007): 6645-6651.

[25] Ahn, B. Y.; Seok, S. I.; and Baek, I. C., Sol-gel microencapsulation of hydrophilic active compounds from the modified silicon alkoxides: The control of pore and particle size. *Materials Science and Engineering: C* 28, 7(2008): 1183-1188.

[26] Lee, S. H.; Kim J. H.; Park J. H.; and Kim S. U., Polymer composite particles containing sunscreen agent and manufacturing method thereof. *Patent Application Publication, US Patent 2009/0053153 A1.* (26 February 2009):

[27] Metha Rutnakornpituk. *Synthesis of silicone magnetic fluids for use in eye surgery*. Doctor of Philosophy. Virginia Polytechnic Institute and State University, 2002.

[28] Coradin, T.; Livage, J., Effect of some amino acids and peptides on silicic acid polymerization. *Colloids and Surfaces B: Biointerfaces* 21, 4(2001): 329-336.

[29] Jang, K. W.; Choi, S. H.; Pyun, S. I.; and John, M. S., The Effects of the Water Content, Acidity, Temperature and Alcohol Content on the Acidic Sol-Gel Polymerization of Tetraethoxysilane (TEOS) with Monte Carlo Simulation. *Molecular Simulation* 27, 1(2001): 1-16.

[30] Deitsch, J. J.; and Smith, J. A., Effect of Triton X-100 on the Rate of Trichloroethene Desorption from Soil to Water. *Environmental Science & Technology* 29, 4(1995): 1069-1080.

[31] European commission enterprise and industry directorate-general. Standardization mandate assigned to CEN concerning. *Methods for testing efficacy of sunscreen products*. Brussels, 2006. (Mimeographed)

APPENDICES

APPENDIX A

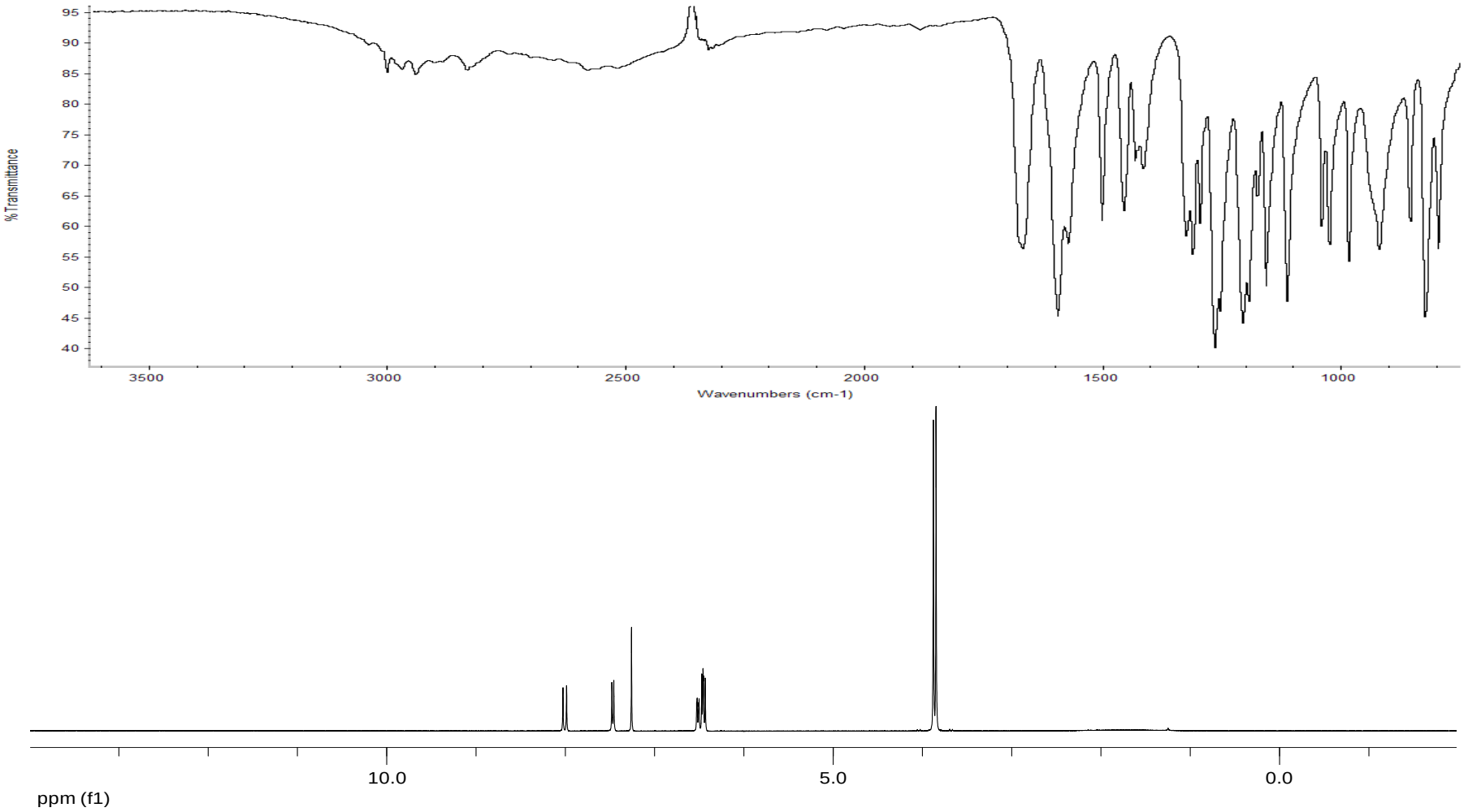

Figure A1 IR (a) and ^{1}H-NMR spectrum (b) of 2,4-dimethoxycinnamic acid **(2,4-DMC)** in $CDCl_3$

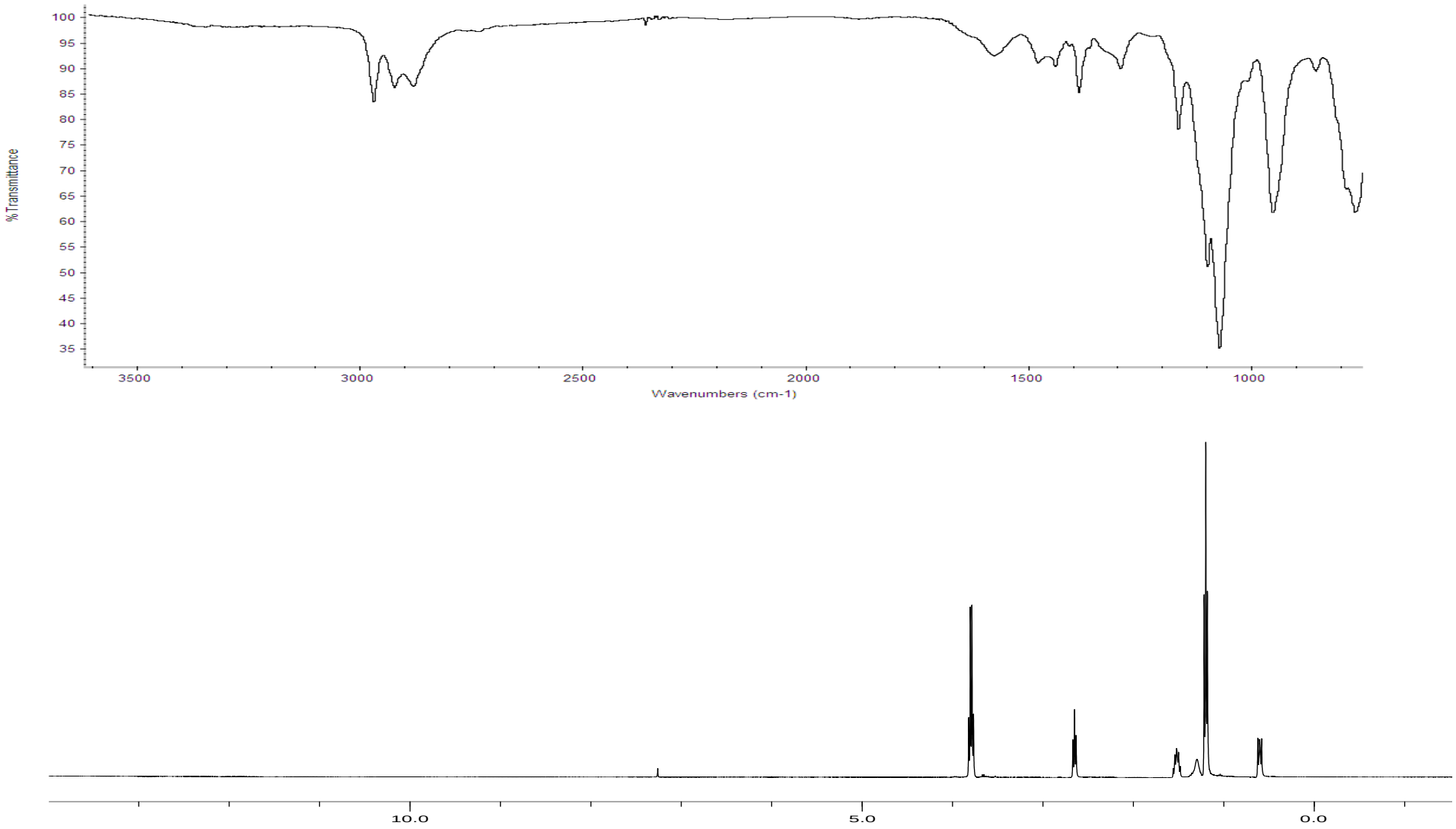

Figure A2 IR (a) and ^{1}H-NMR spectrum (b) of 3-aminopropyltriethoxysilane **(APTES)** in $CDCl_3$

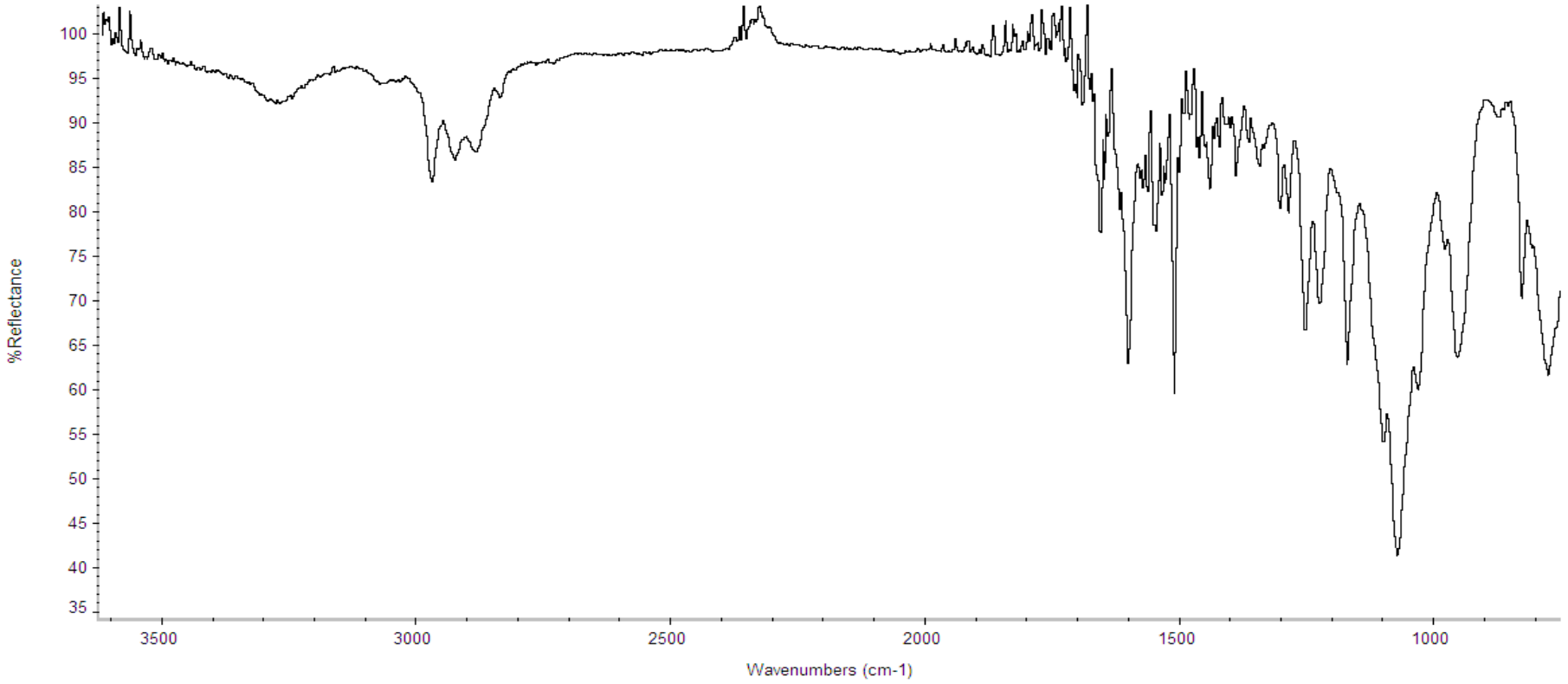

Figure A3 IR spectrum of triethoxysilylpropyl-4-methoxycinnamamide, DS=0.8 **(TES4C-2)** in $CDCl_3$

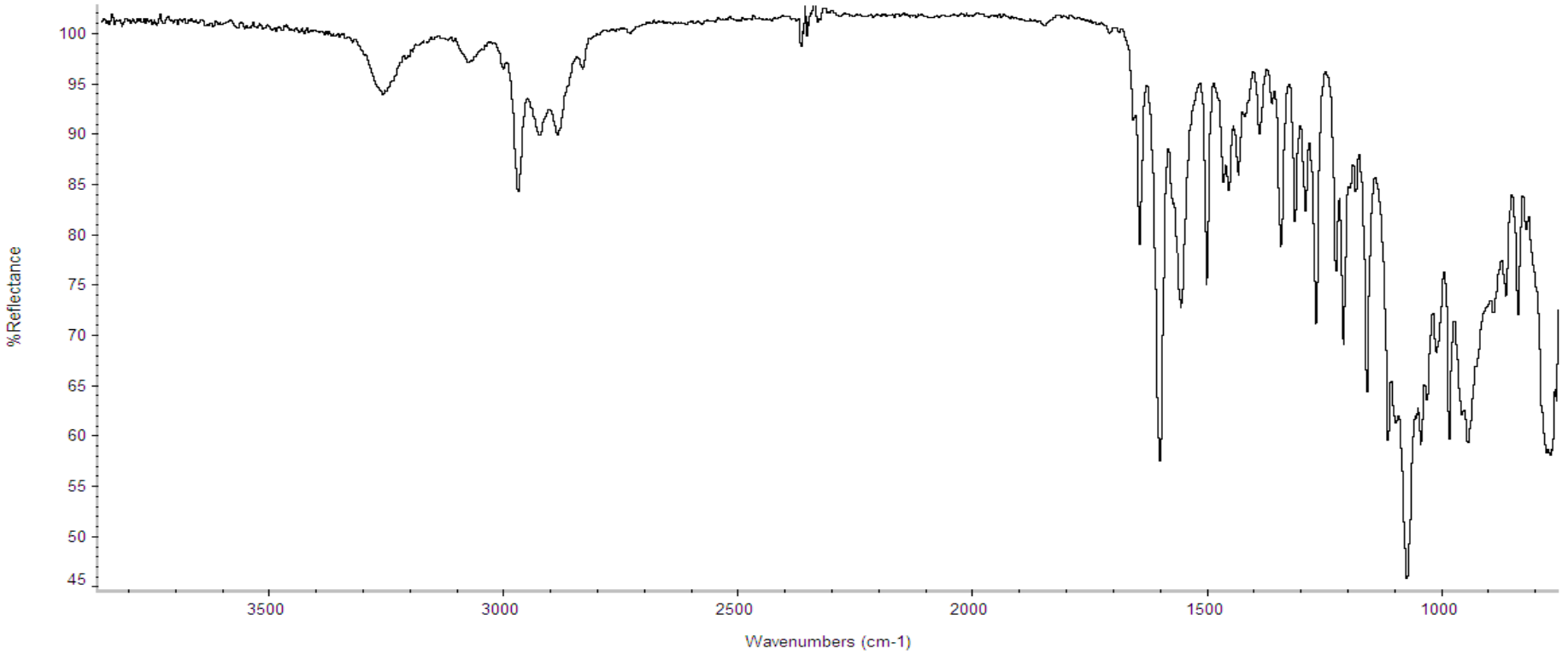

Figure A4 IR spectrum of triethoxysilylpropyl-2,4-dimethoxycinnamamide, DS=0.78 **(TES24C-2)** in $CDCl_3$

I. Poly[propyl-4-methoxycinnamamidesilsesquioxane] (PTES4C) spheres

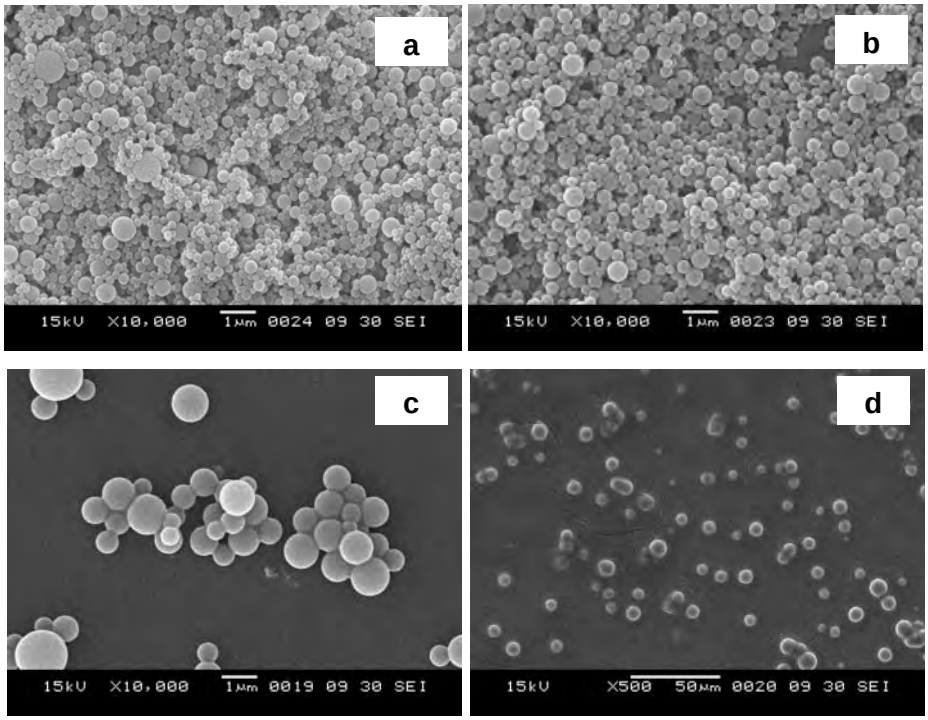

Figure A5 Scanning electron micrographs of **PTES4C** spheres prepared under self-catalytic process at 0.02 g/ml monomer concentration with the ethanol percentages of 10% (v/v) (a), 20% (v/v) (b), 30% (v/v) (c) and 40% (v/v) (d).

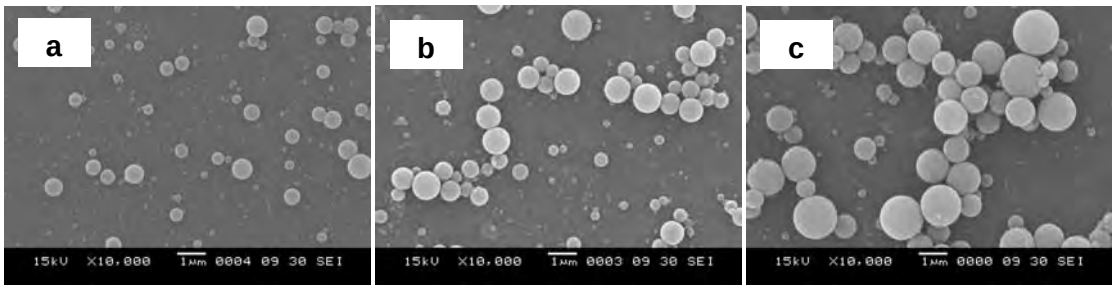

Figure A6 Scanning electron micrographs of **PTES4C** spheres prepared under 0.1% HCl catalytic process at 0.02 g/ml monomer concentration with the ethanol percentages of 20% (v/v) (a), 30% (v/v) (b) and 40% (v/v) (c).

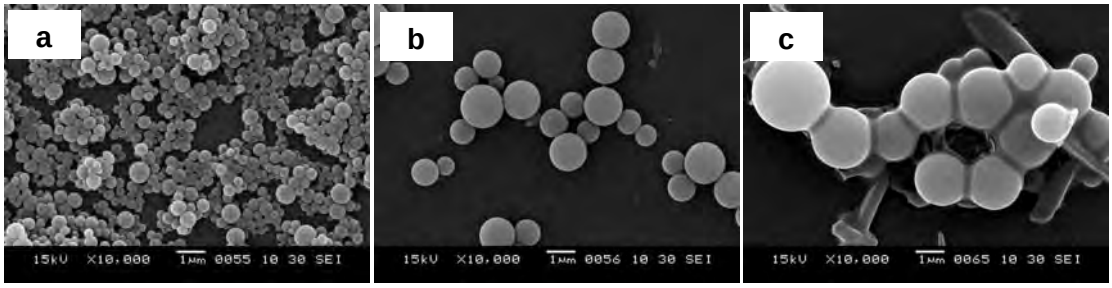

Figure A7 Scanning electron micrographs of **PTES4C** spheres prepared under 3% NH_4OH catalytic process at 0.02 g/ml monomer concentration with the ethanol percentages of 20% (v/v) (a), 30% (v/v) (b) and 40% (v/v) (c).

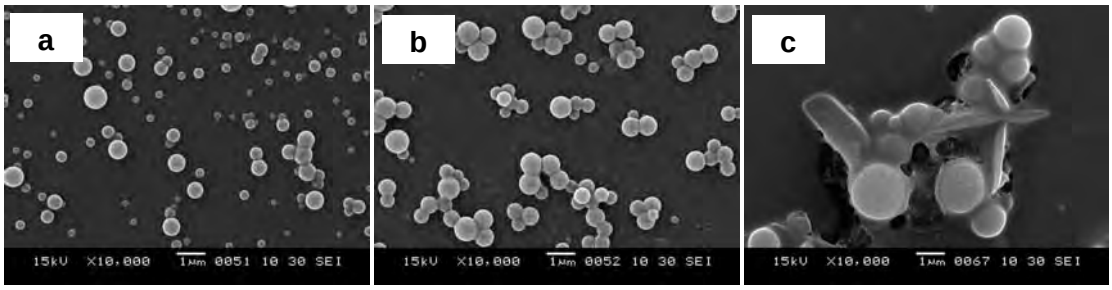

Figure A8 Scanning electron micrographs of **PTES4C** spheres prepared under **5**% NH_4OH catalytic process at 0.02 g/ml monomer concentration with the ethanol percentages of 20% (v/v) (a), 30% (v/v) (b) and 40% (v/v) (c).

II. 3.2.2 Poly[propyl-2,4-dimethoxycinnamamidesilsesquioxane] (PTES24C) spheres

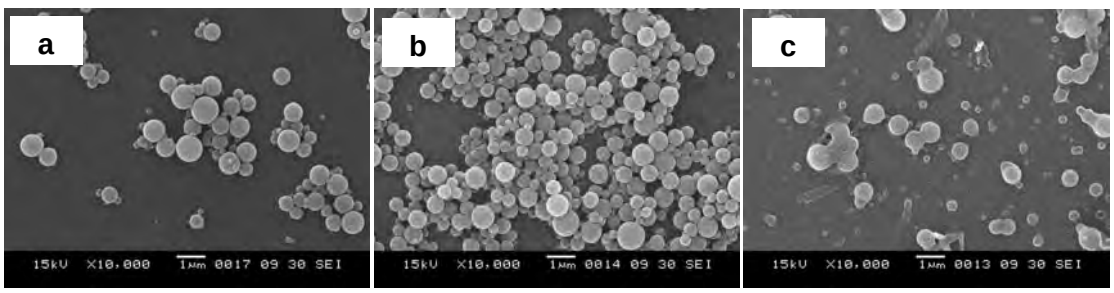

Figure A9 Scanning electron micrographs of **PTES24C** spheres prepared under 0.1% HCl catalytic process at 0.02 g/ml monomer concentration with the ethanol percentages of 10% (v/v) (a), 20% (v/v) (b) and 30% (v/v) (c).

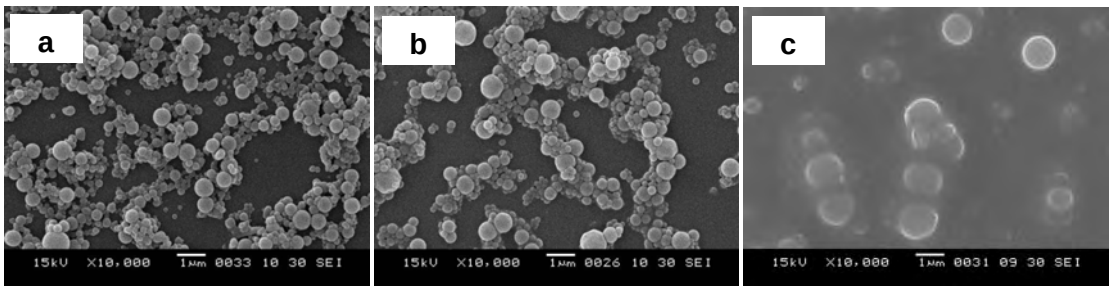

Figure A10 Scanning electron micrographs of **PTES24C** spheres prepared under self-catalytic catalytic process at 0.02 g/ml monomer concentration with the ethanol percentages of 10% (v/v) (a), 20% (v/v) (b) and 30% (v/v) (c).

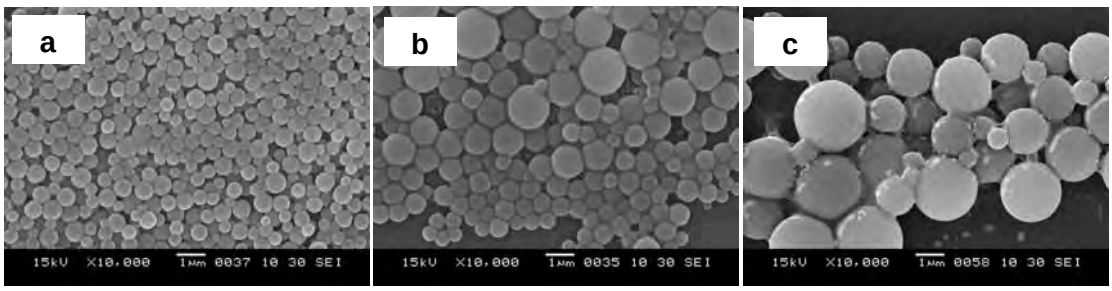

Figure A11 Scanning electron micrographs of **PTES24C** spheres prepared under 3% NH_4OH catalytic process at 0.02 g/ml monomer concentration with the ethanol percentages of 10% (v/v) (a), 20% (v/v) (b) and 30% (v/v) (c).

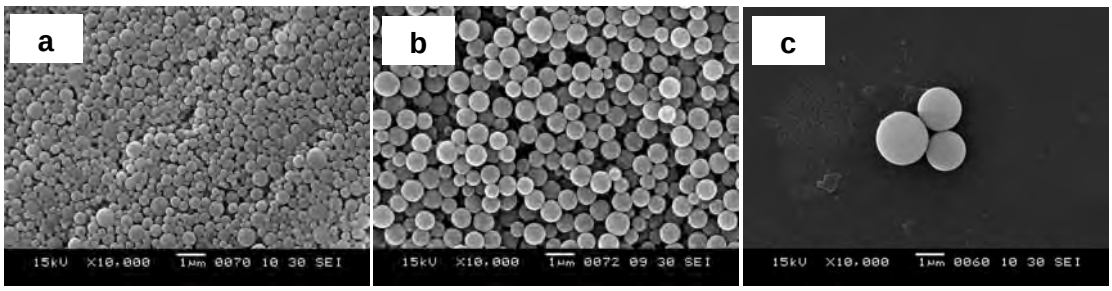

Figure A12 Scanning electron micrographs of **PTES24C** spheres prepared under 5% NH_4OH catalytic process at 0.02 g/ml monomer concentration with the ethanol percentages of 10% (v/v) (a), 20% (v/v) (b) and 30% (v/v) (c).

APPENDIX B

I. Content of EHMC loaded into particle PTES4C-2

In 5 ml of initially sample

- Weight of the **EHMC**-encapsulated **PTES4C-2** particles = 0.1534 g
- Weight of **EHMC** initially used = 0.0520 g

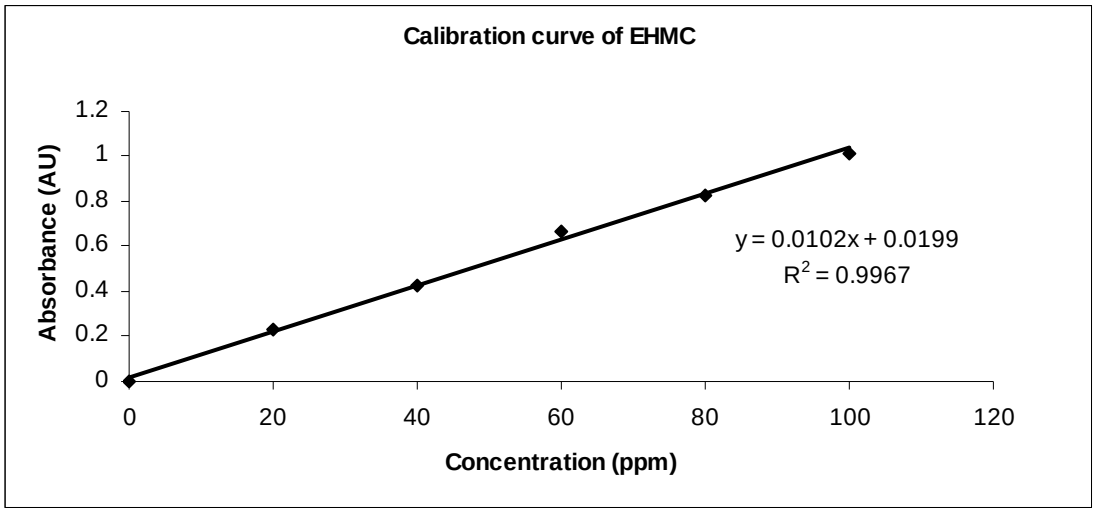

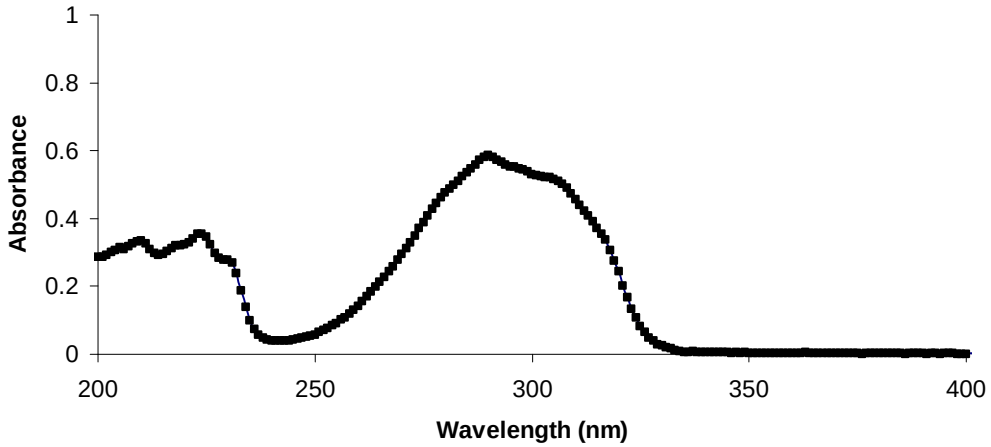

From the equation of calibration curve:

y = 0.0102x + 0.0199, R^2= 0.9967

0.455 = 0.0102x + 0.0199

X = 42.6568

∴ Weight of EHMC in the **PTES4C-2** particle 42.6568 ppm

ppm → mg/ L = 42.6568 mg/ L

In volumetric 10 x $l0^{-3}$ L gave content of **EHMC** in the **PTES4C-2** particle

= 0.4265 mg = 4.2656 x 10^{-4} g

In the 0.2 ml hexane extracted

$$C_1V_1 = C_2V_2$$

$$\frac{4.2656 \times 10^{-4} \times 1000}{290.4\ (MW_{EHMC})} = C_2 \times 0.2$$

$$C_2 = 7.3445 \times 10^{-3}\ mol/L$$

∴ Weight **EHMC** from the 15 ml hexane extracted

= 0.0320 g

% Loading capacity

$$= \frac{\text{weight of encapsulated } \textbf{EHMC} \text{ in the particles} \times 100}{\text{weight of } \textbf{EHMC}\text{-encapsulated particles}}$$

$$= \frac{0.0320 \times 100}{0.1534}$$

Therefore, from the calculation determined that % loading capacity of **EHMC** is

= 20.86%

% Encapsulation efficiency

$$= \frac{\text{weight of encapsulated } \textbf{EHMC} \text{ in the particles} \times 100}{\text{weight of } \textbf{EHMC} \text{ initially used}}$$

$$= \frac{0.0320 \times 100}{0.0520}$$

Therefore, from calculation determined that % encapsulation efficiency of **EHMC** is

= 61.54%

II. Content of EHMC loaded into particle PTES24C-2

In 5 ml of initially sample

- Weight of the **EHMC**-encapsulated **PTES24C-2** particles = 0.1569 g
- Weight of **EHMC** initially used = 0.0502 g

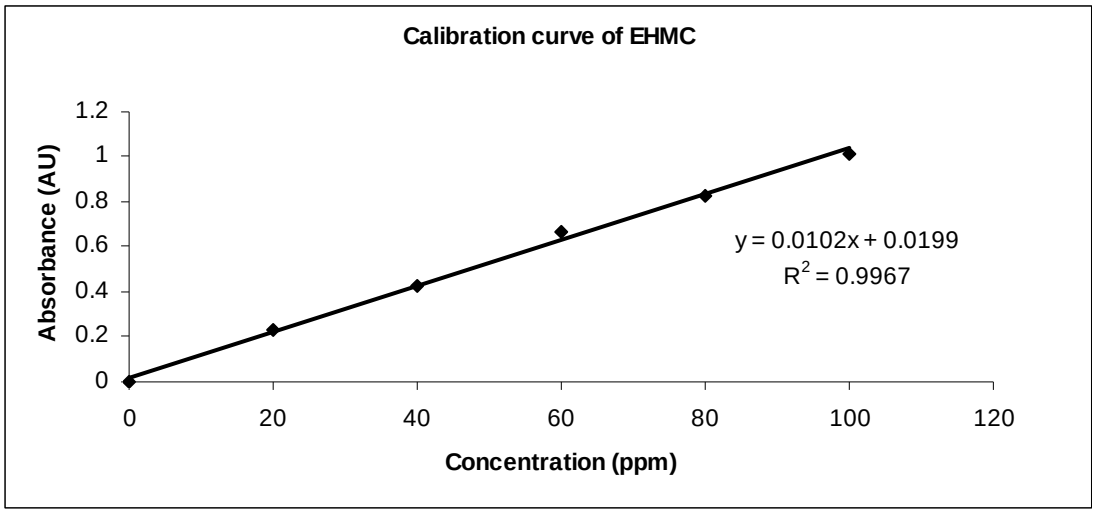

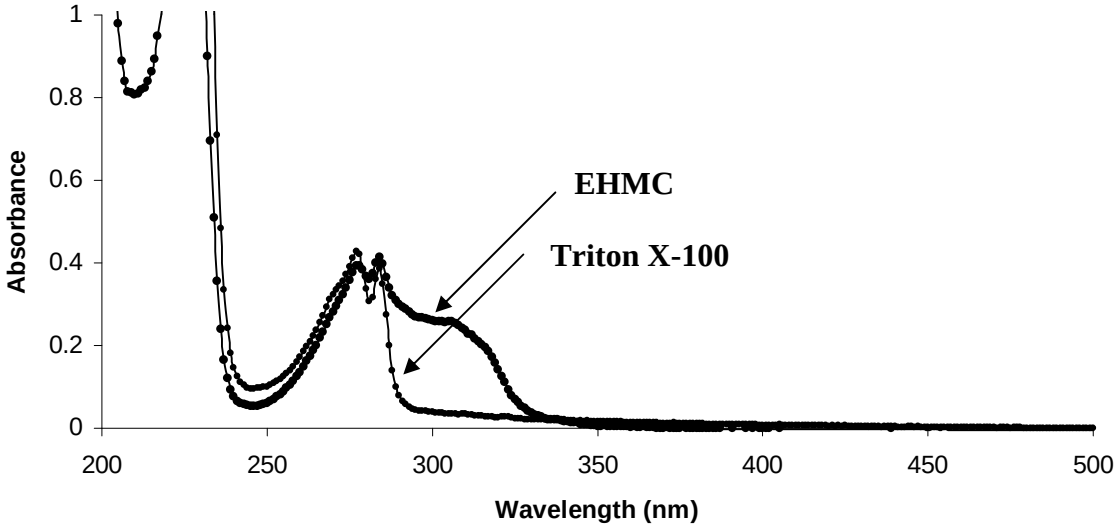

From the equation of calibration curve:

y = 0.0102x + 0.0199, R^2= 0.9967

0.237 = 0.0102x + 0.0199

X = 21.2843

.∴ Weight of EHMC in the **PTES24C-2** particle 21.2843 ppm

ppm → mg/ L = 21.2843 mg/ L

In volumetric 10 x $l0^{-3}$ L gave content of **EHMC** in the **PTES24C-2** particle

= 0.2128 mg = 2.1284 x 10^{-4} g

In the 0.2 ml hexane extracted

$$C_1V_1 = C_2V_2$$

$$\frac{2.1284 \times 10^{-4} \times 1000}{290.4\ (MW_{EHMC})} = C_2 \times 0.2$$

$$C_2 = 3.6646 \times 10^{-3}\ mol/L$$

.∴ Weight **EHMC** from the 15 ml hexane extracted

= 0.0160 g

% Loading capacity

$$= \frac{\text{weight of encapsulated } \mathbf{EHMC} \text{ in the particles x 100}}{\text{weight of } \mathbf{EHMC}\text{-encapsulated particles}}$$

$$= \frac{0.0160 \times 100}{0.1569}$$

Therefore, from the calculation determined that % loading capacity of **EHMC** is

= 10.17%

% Encapsulation efficiency

$$= \frac{\text{weight of encapsulated } \mathbf{EHMC} \text{ in the particles x 100}}{\text{weight of } \mathbf{EHMC} \text{ initially used}}$$

$$= \frac{0.0160 \times 100}{0.0502}$$

Therefore, from calculation determined that % encapsulation efficiency of **EHMC** is

= 31.87%

VITA

Ms. Punnipa Kidsaneepoiboon was born on March 31, 1984 in Bangkok, Thailand. She got a Bachelor's Degree of Science in Chemistry from Chulalongkorn University After that, she started her graduated study a Master's Degree in Organic Chemistry at Chulalongkorn University and completed program in 2009.

Her address is 12/108 Ngamwongwan Road, Jatujak, Bangkok, 10900, Tel. 02-953-0478, 089-882-3990